Quantum technologies based on nitrogen-vacancy centers in diamond: towards applications in (quantum) biology

Jianming Cai

Institute of Theoretical Physics, Universität Ulm

2013-03-02

Alexander von Humboldt Stiftung / Foundation

DFG Deutsche Forschungsgemeinschaft

MARIE CURIE ACTIONS

Institute of Theoretical Physics, Ulm University

Martin Plenio
Alex Retzker (The Hebrew University of Jerusalem)
Jianming Cai

Institute of Quantum Optics, Ulm University

Fedor Jelezko

Boris Naydenov
Kay Jahnke

Liam P. McGuinness
Rainer Pfeiffer

Paz London
Jochen Scheue

Spin properties of NV-center

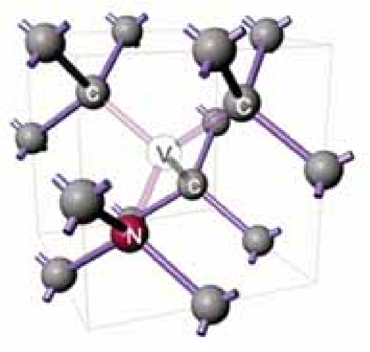

- ⦿ Color centers in diamond
- ⦿ Single point defects in a crystalline matrix
- ⦿ A carbon vacancy migrate and bounds to Nitrogen
- ⦿ Atomic emitter – can be shrunk to nm sized
- ⦿ Non-toxic: biological and medical applications

- Spin polarization via optical pumping

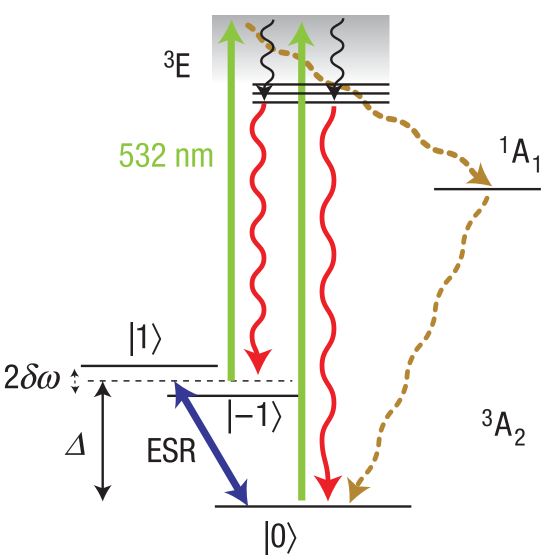

M. D. Liukin (Harvard)

- Optical read out of spin state

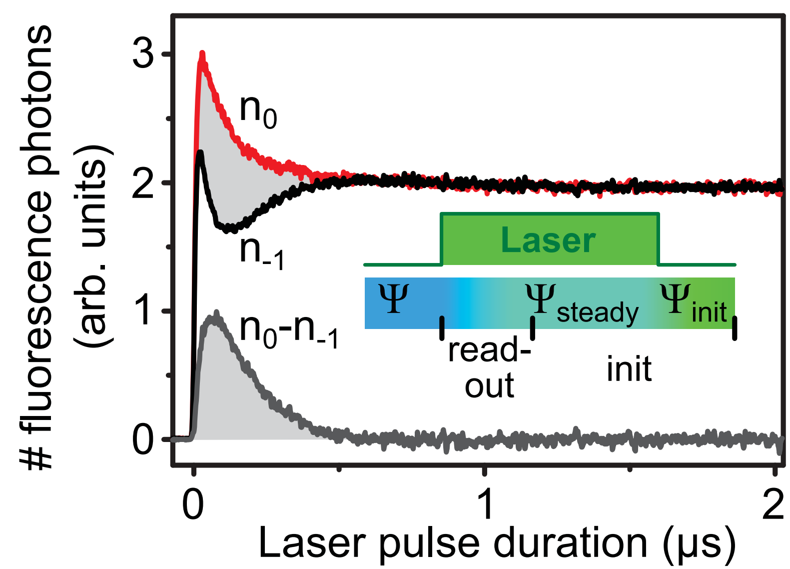

P. Neumann thesis (2012)

Spin properties of NV-center

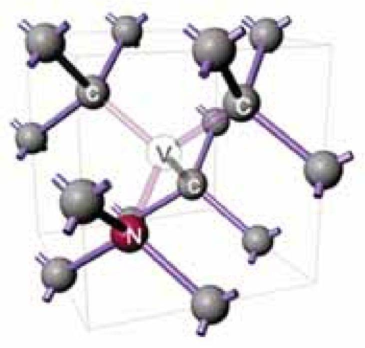

- ⦿ Color centers in diamond
- ⦿ Single point defects in a crystalline matrix
- ⦿ A carbon vacancy migrate and bounds to Nitrogen
- ⦿ Atomic emitter – can be shrunk to nm sized
- ⦿ Non-toxic: biological and medical applications

- Spin polarization via optical pumping

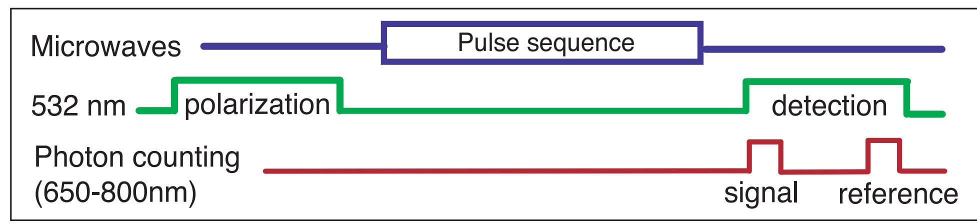

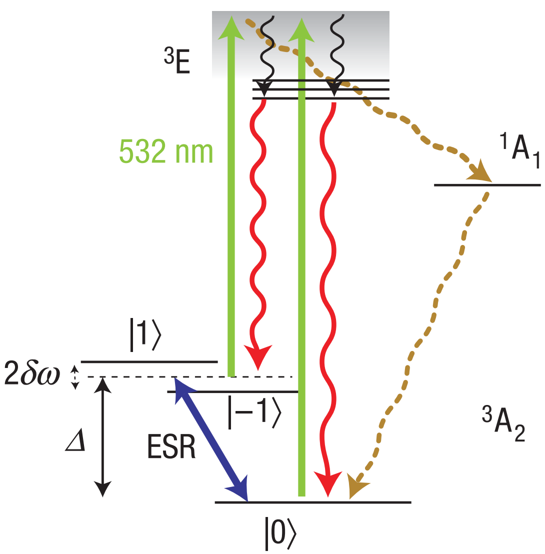

M. D. Liukin (Harvard)

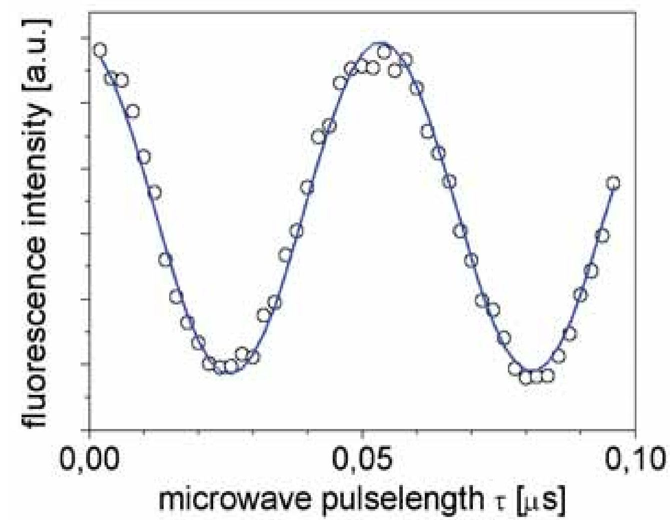

A. Gruber et al., Science 276, 2012 (1997)

NV^- production

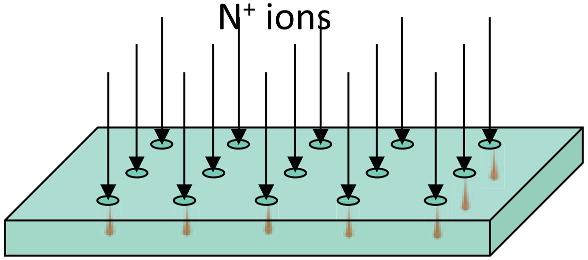

❍ Implantation of nitrogen ions: vacancies

❍ Annealing at T > 700 °C: migration of vacancies → creations of NV centers

❍ Cleaning the surface in acid

Yield depends on the implantation energy 1 to 60 %

J. Meijer et. al., APL 87, 261909 (2005). J. R. Rabeau, et al. APL 88, 023113 (2006)

Point defect with single emitter

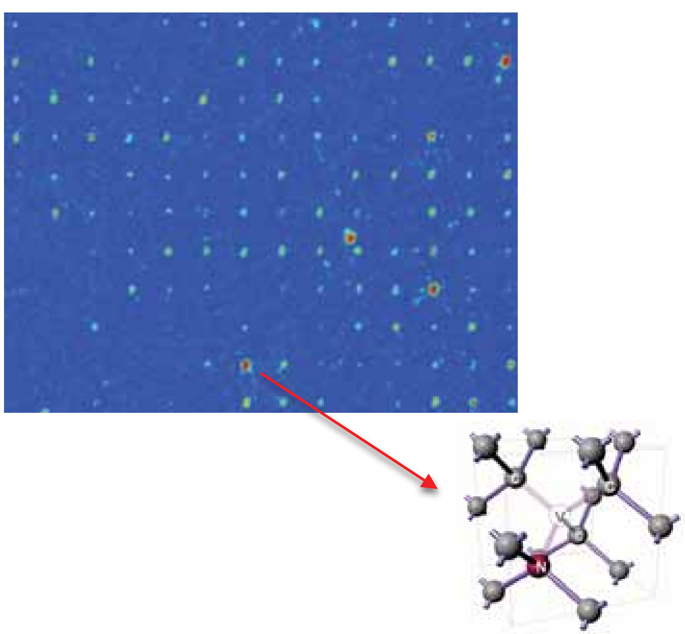

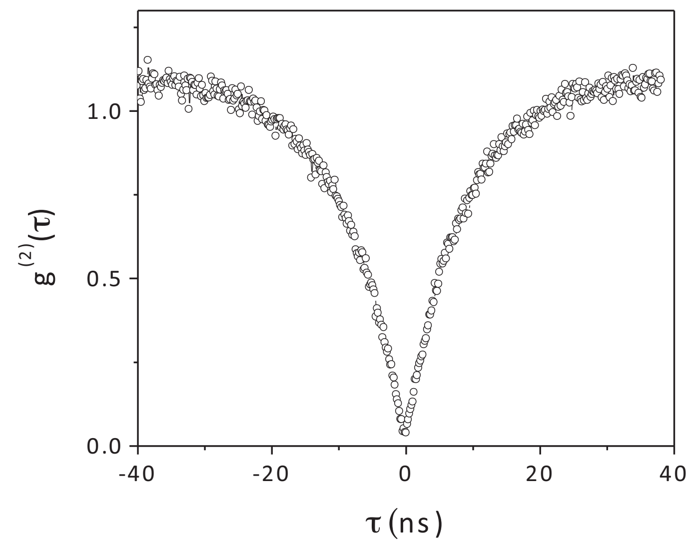

quantum computing

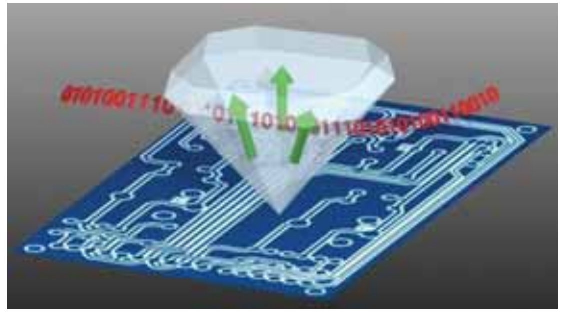

P. Neumann et al., *Science* *329, 542 (2010)*

Scanning probe magnetometer

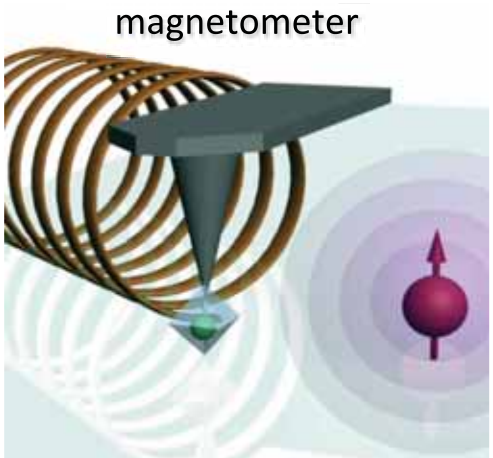

Quantum devices and photonics

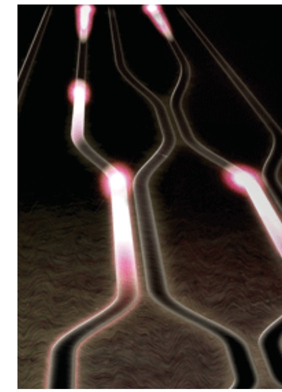

G. Balasubramanian, et al. *Nature* 455, 648 (2008)
J.Maze, et al, Nature 455, 644 (2008)

R. Kolesov et al. *Nat. Phys.* 5, 470 (2009)

Nanodiamonds for cellular imaging

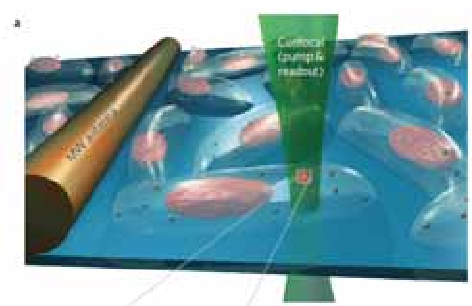

NV in diamond

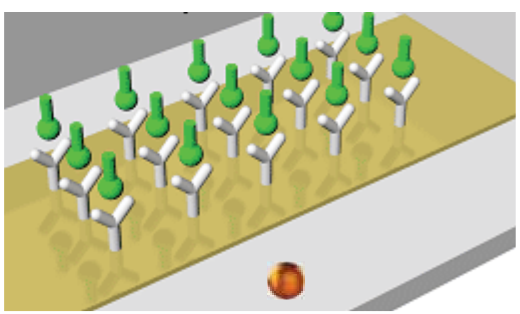

Biosensor technology & Molecular Spin sensors

L. C. L. Hollenberg, et al, Nature Nanotec 6, 358 (2011).

Slide from Boris Naydenov

NV in diamond

Decoherence of NV centers in diamond

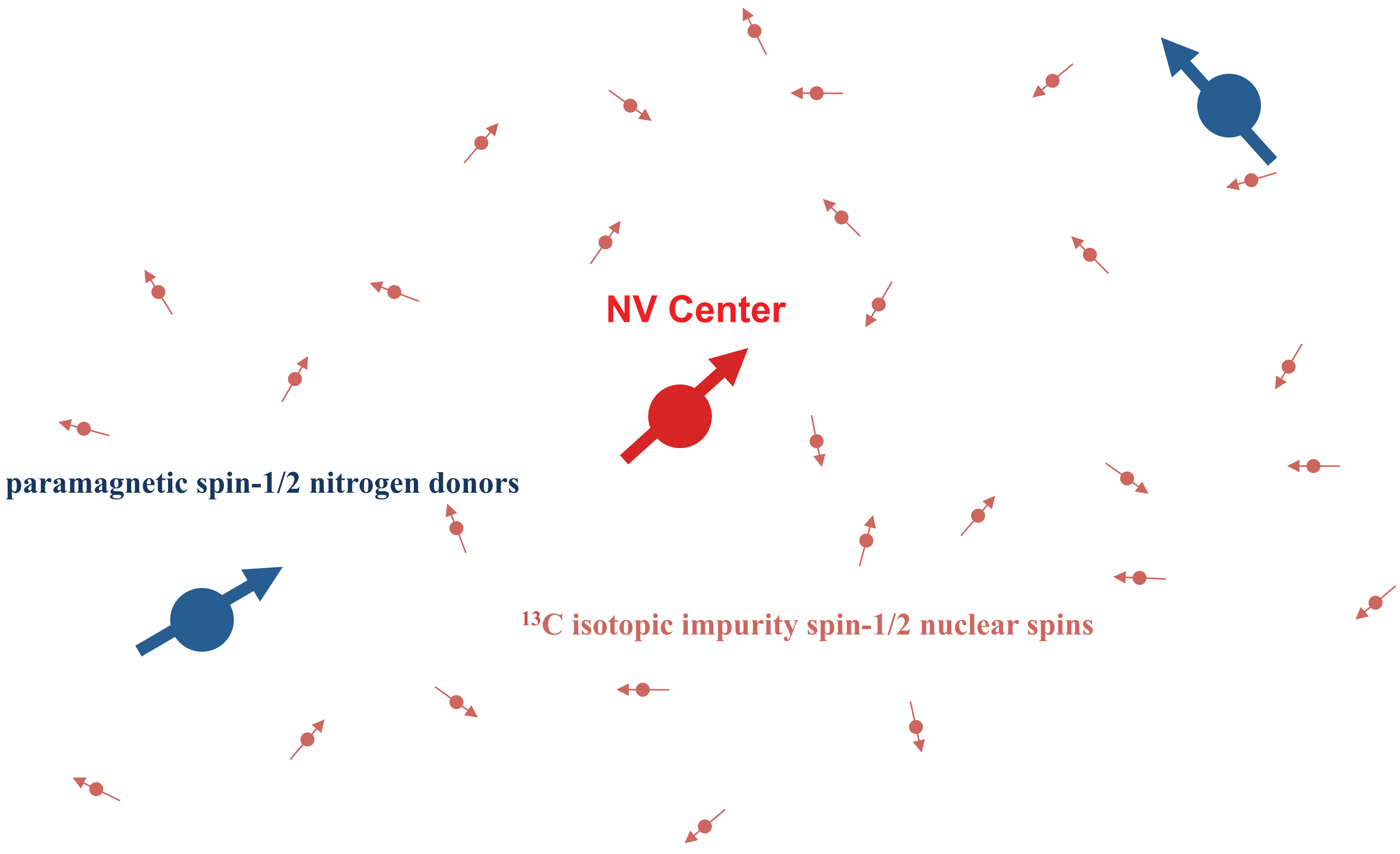

NV$^-$ production

NIMS
Tsukuba

99.999% ^{12}C Enrichment

growth of ^{12}C enriched single crystal diamond starting from 99.999% ^{12}C enriched CH_4

^{12}C 99.995%
(SIMS, EPR)

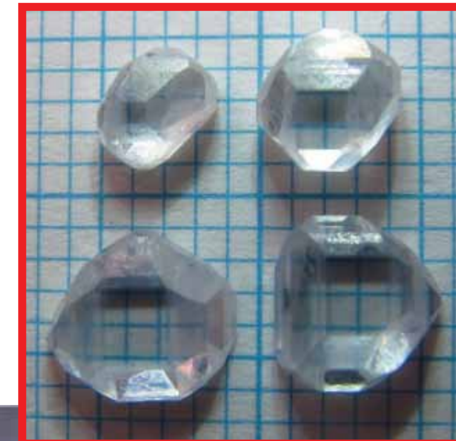

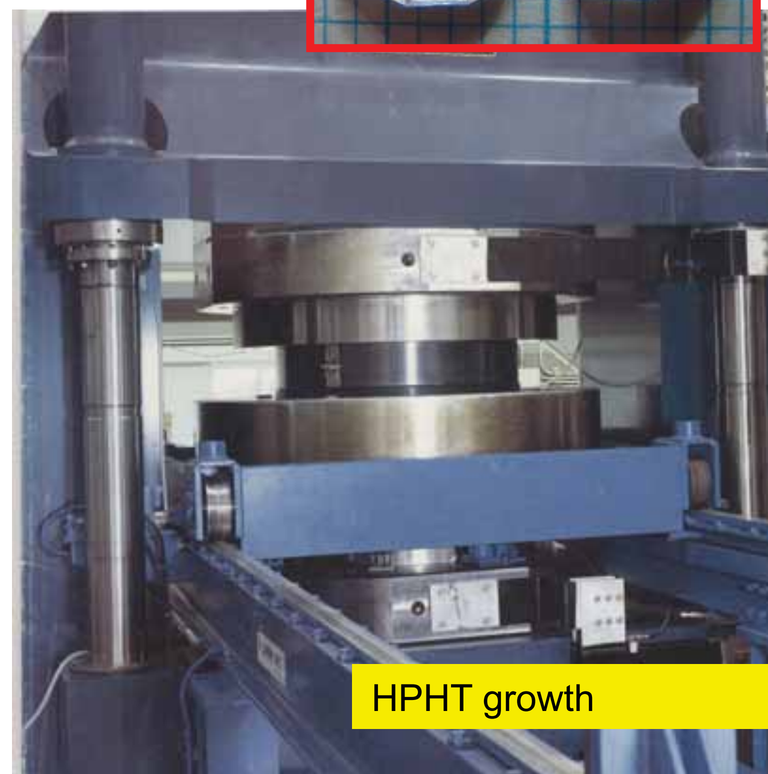

HPHT growth

CVD growth

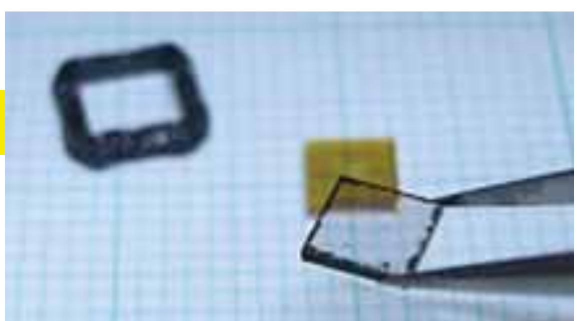

^{12}C 99.998%
(SIMS)

NV^- production

Isotope: 99.999% ^{12}C

Concentration of impurities: below 10^{12} cm-3

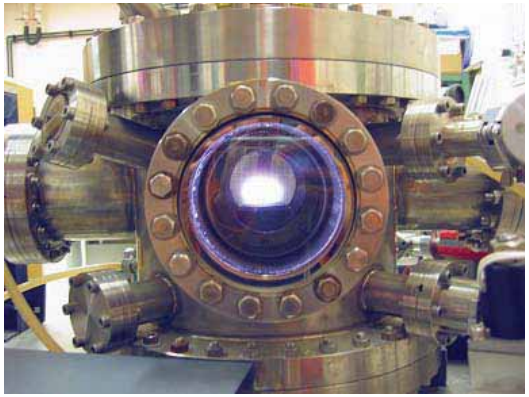

CVD reactor: University Paris XIII (Villtaneuse) J. Achard

D. Twitchen, Element 6 Ltd

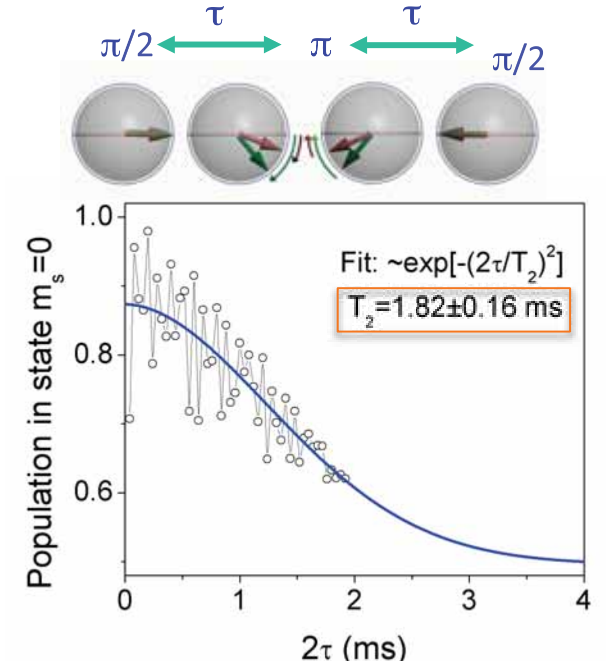

G. Balasubramanian, et.al Nature Materials 8, 383 (2009)

Engineering shallow NV centers s in diamond

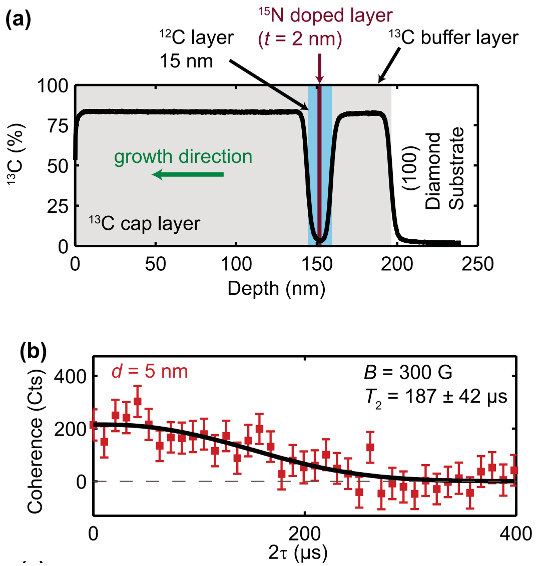

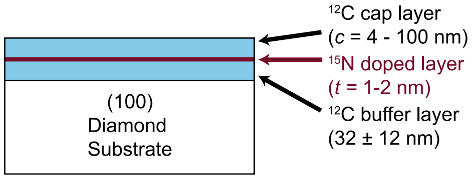

David D. Awschalom (UCSB), APL (2012)

Quantum metrology with NV center: atomic-sized magnetometer

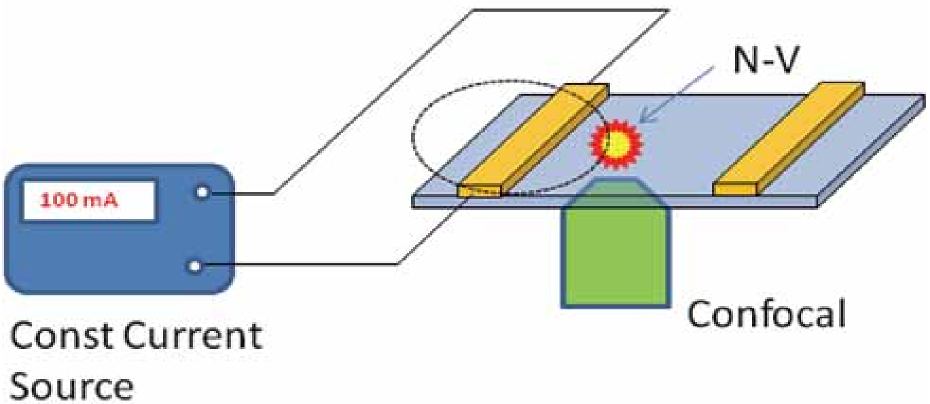

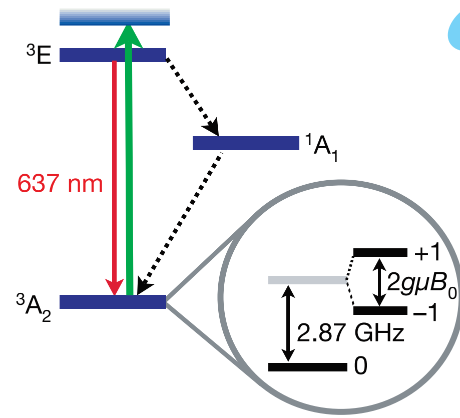

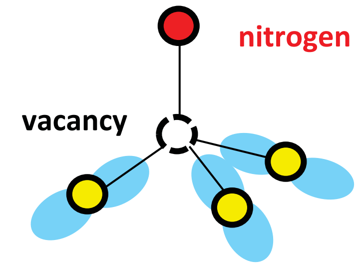

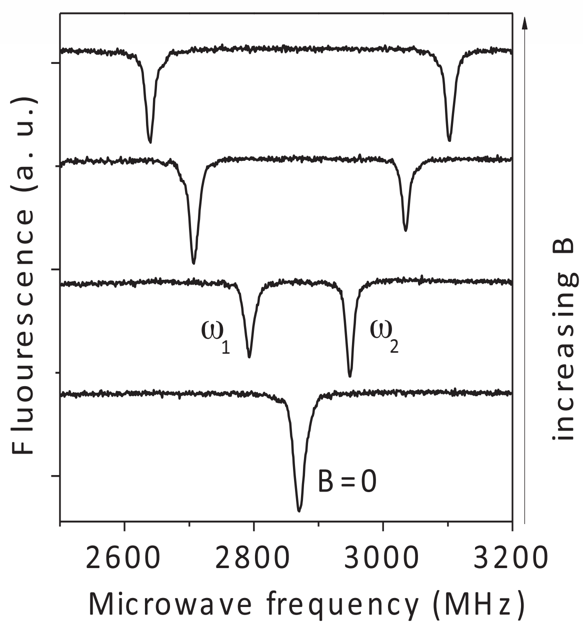

- Zeeman effect on single spin
- Sensitivity depends on the line width

Stuttgart group, Nature (2008)

Quantum metrology with NV center: atomic-sized magnetometer

Lukin group, Nature (2008)

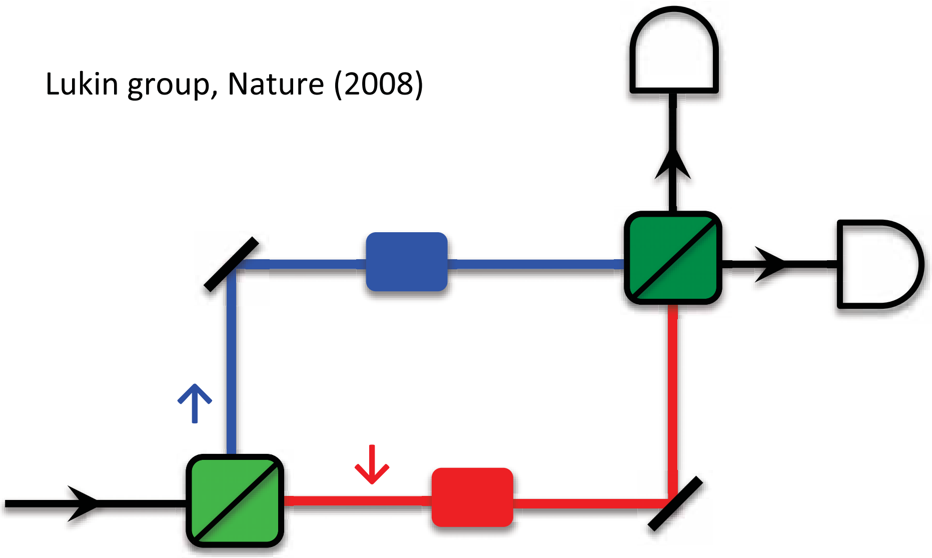

Static magnetic field

- Shot noise limit sensitivity

$$\eta = \frac{\langle \Delta P^2 \rangle^{1/2}}{\partial P / \partial b} = \frac{\hbar}{g\mu_B t} \qquad P = \cos^2\left(\frac{bt}{2}\right) = \frac{1}{2}\left[1+\cos(bt)\right]$$

$$\Downarrow$$

$$P = \frac{1}{2}\left[1+\cos(bt)\, f(t)\right]$$

- Sensitivity depends on T_2^*

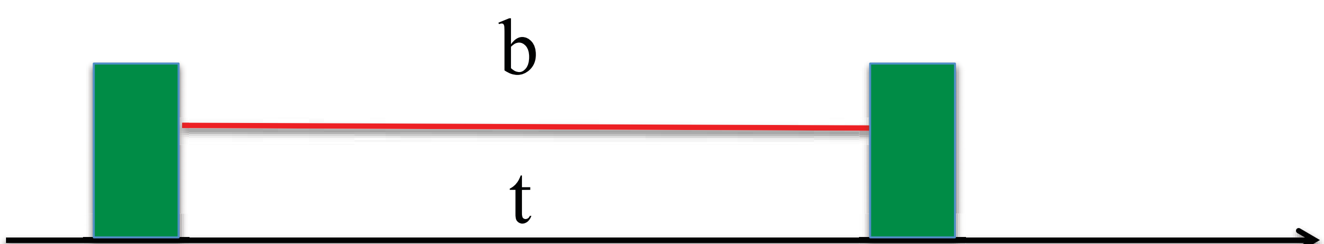

$\uparrow \longrightarrow \uparrow + \downarrow \longrightarrow e^{-ibt/2}\uparrow + e^{ibt/2}\downarrow \longrightarrow \cos(bt/2)\uparrow - i\sin(bt/2)\downarrow$

Quantum metrology with NV center: atomic-sized magnetometer

Lukin group, Nature (2008)

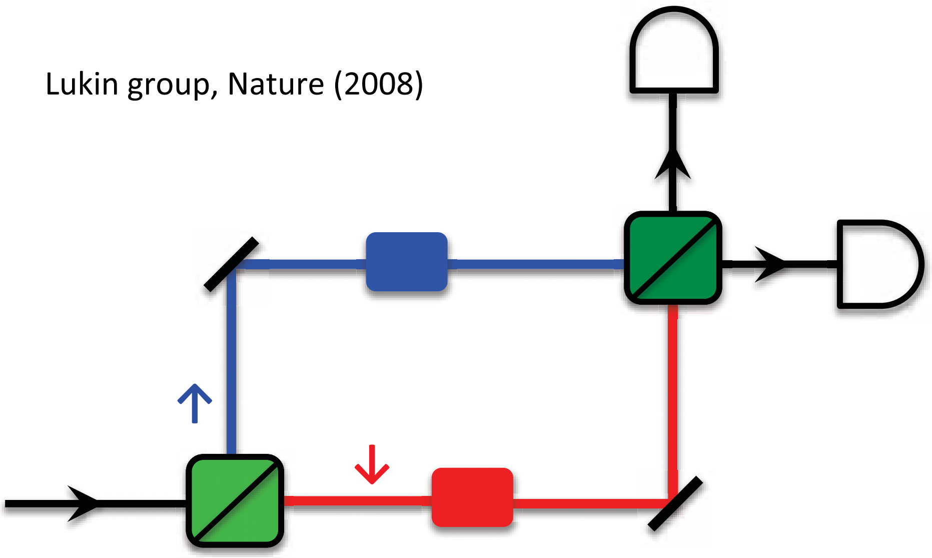

- Shot noise limit sensitivity

$$\eta = \frac{\langle \Delta P^2 \rangle^{1/2}}{\partial P / \partial b} = \frac{\hbar}{g \mu_B t} \qquad P = \cos^2\left(\frac{bt}{2}\right) = \frac{1}{2}\left[1 + \cos(bt)\right]$$

$$\Downarrow$$

$$P = \frac{1}{2}\left[1 + \cos(bt) f(t)\right]$$

- Sensitivity depends on T_2^*

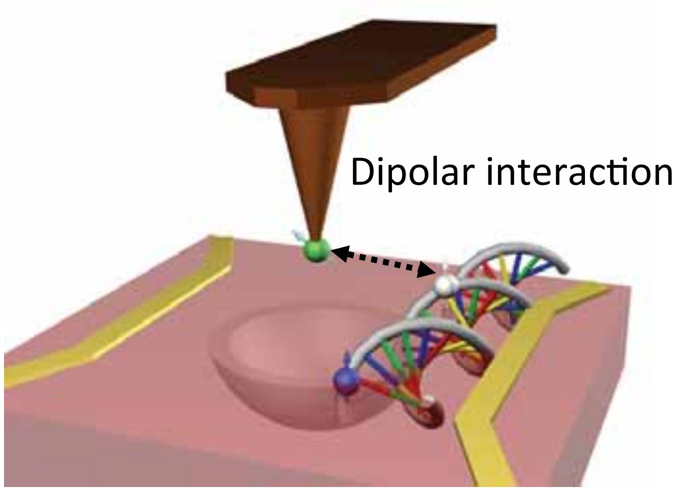

$$B = \frac{\mu_0 \hbar \gamma_e}{r^3}\left[1 - 3\cos^2(\theta)\right] S_z$$

Spin	Distance (r)	Field	Required T_2
Electron	10 nm	1μT	~ 2 μs
Proton	10 nm	1nT	~ 2 ms

Quantum metrology with NV center: atomic-sized magnetometer

AC magnetic field

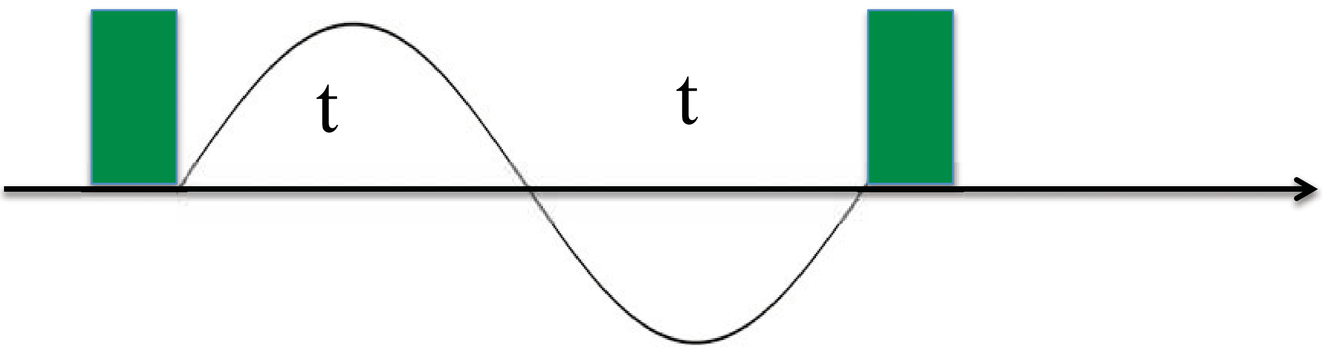

$$\uparrow \longrightarrow \uparrow + \downarrow \longrightarrow e^{-ix}\uparrow + e^{ix}\downarrow \longrightarrow \uparrow + \downarrow \longrightarrow \uparrow$$

Quantum metrology with NV center: atomic-sized magnetometer

AC magnetic field

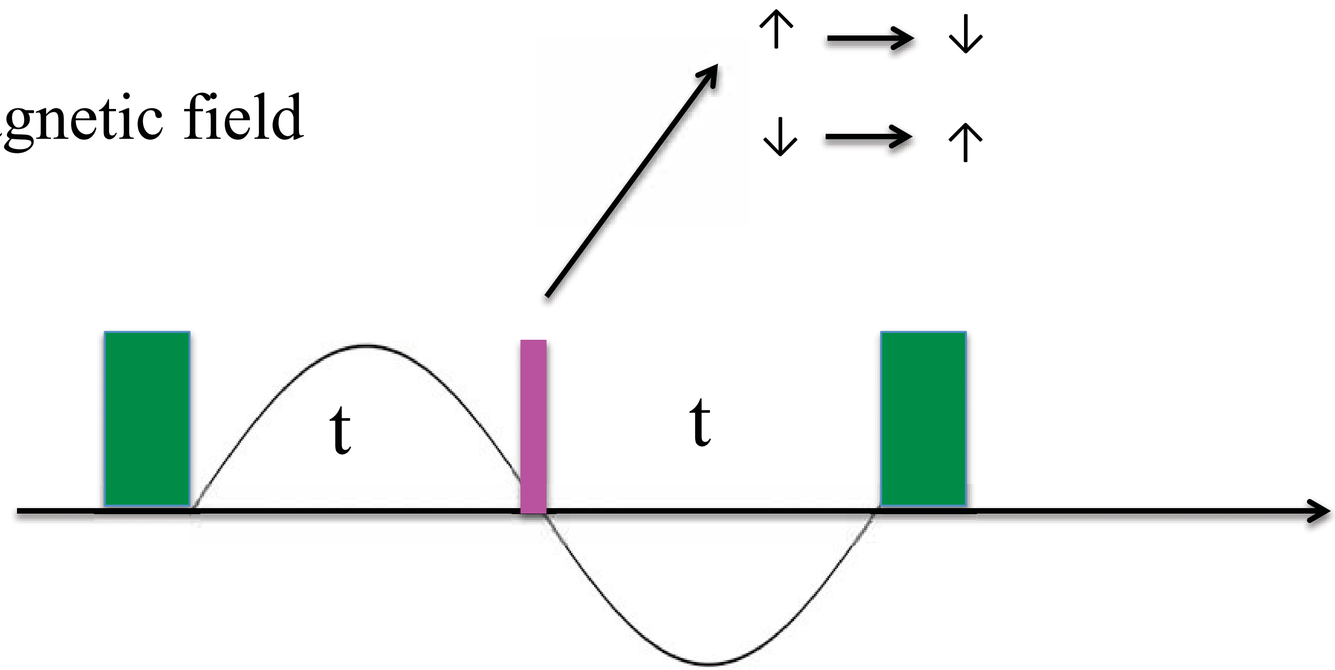

$\uparrow \longrightarrow \uparrow + \downarrow \longrightarrow$ $e^{ix}\uparrow + e^{-ix}\downarrow$

$e^{ix}\downarrow + e^{-ix}\uparrow$

$e^{i2x}\downarrow + e^{-i2x}\uparrow$ $\longrightarrow \cos(2x)\uparrow - i\sin(2x)\downarrow$

Quantum metrology with NV center: atomic-sized magnetometer

DC magnetic field

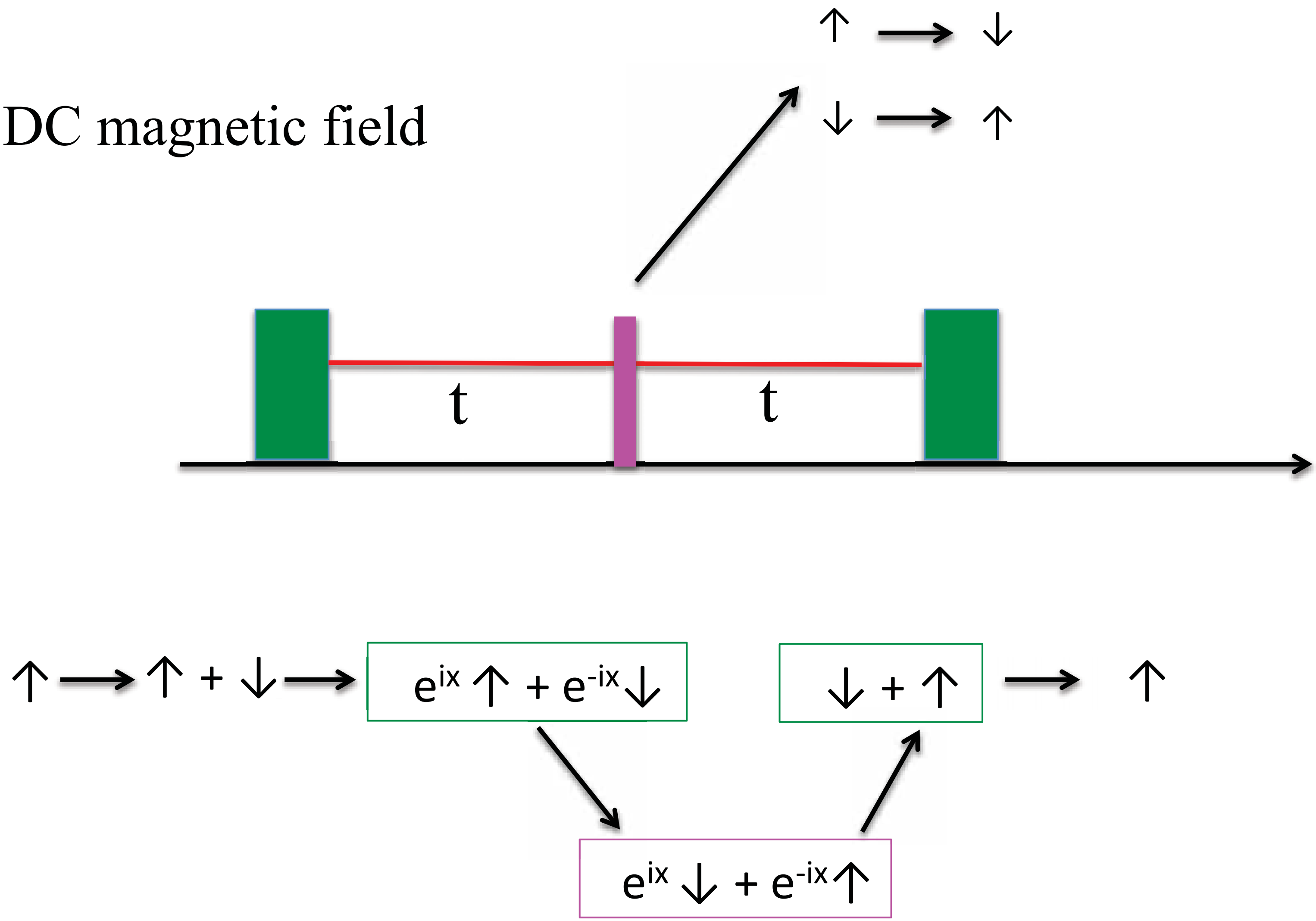

Quantum metrology with NV center: atomic-sized magnetometer

$$\hat{H} = \frac{1}{2}[\Omega + \beta(t)]\hat{\sigma}_z$$

Decay of coherence:

$$W(t) \equiv e^{-\chi(t)}$$

$$\chi(t) = \int_0^\infty \frac{d\omega}{\pi} S(\omega) \frac{F(\omega t)}{\omega^2}$$

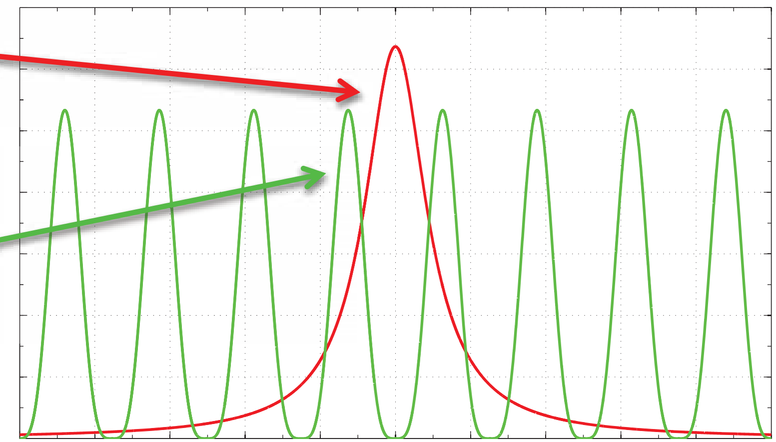

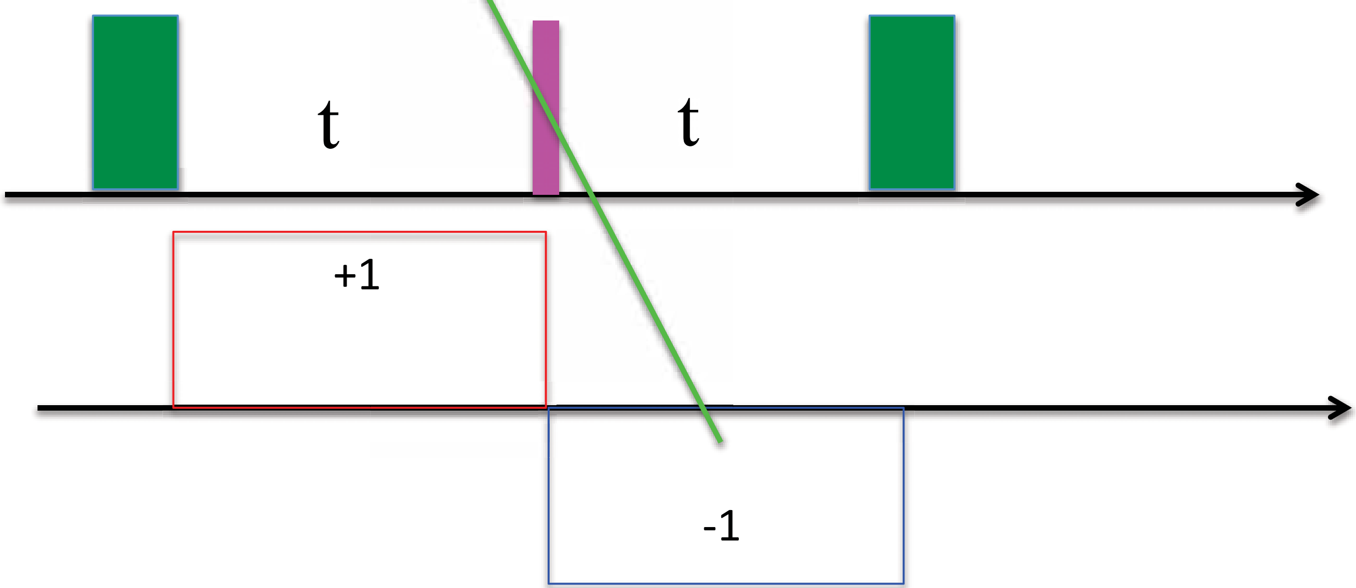

Quantum metrology with NV center: atomic-sized magnetometer

$$\hat{H} = \frac{1}{2}[\Omega + \beta(t)]\hat{\sigma}_z$$

Decay of coherence:

$$W(t) \equiv e^{-\chi(t)}$$

$$\chi(t) = \int_0^\infty \frac{d\omega}{\pi} S(\omega) \frac{F(\omega t)}{\omega^2}$$

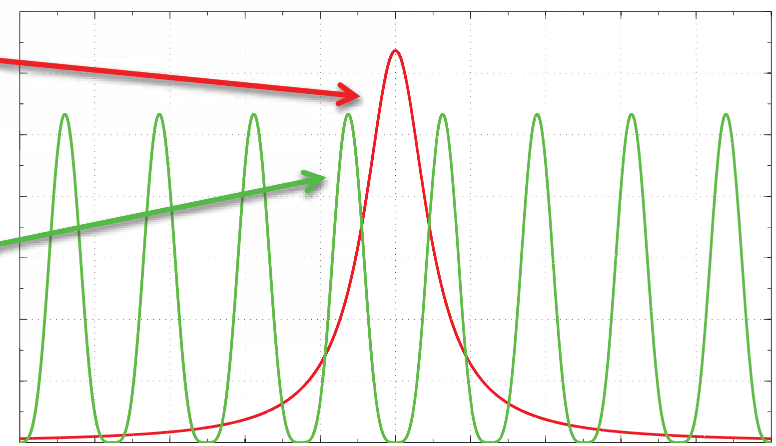

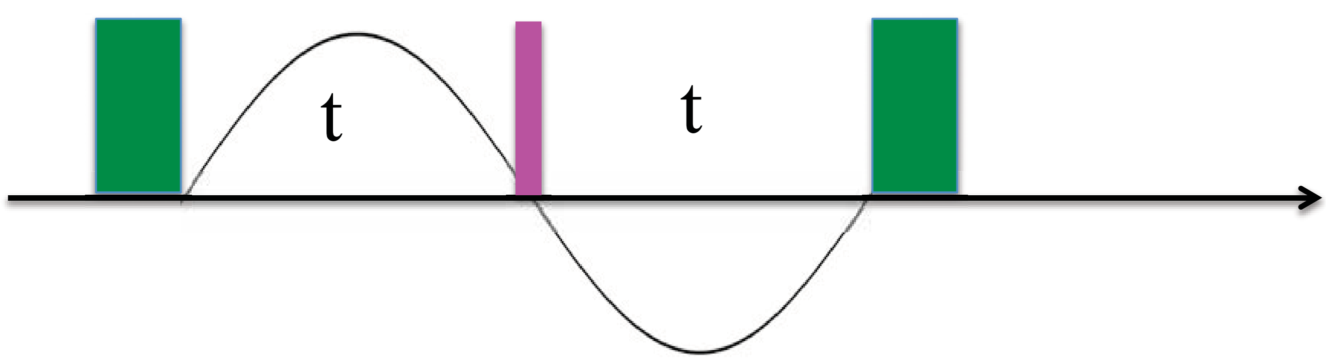

Quantum metrology with NV center: atomic-sized magnetometer

$$\hat{H} = \frac{1}{2}[\Omega + \beta(t)]\hat{\sigma}_z$$

Decay of coherence:

$$W(t) \equiv e^{-\chi(t)}$$

$$\chi(t) = \int_0^\infty \frac{d\omega}{\pi} S(\omega) \frac{F(\omega t)}{\omega^2}$$

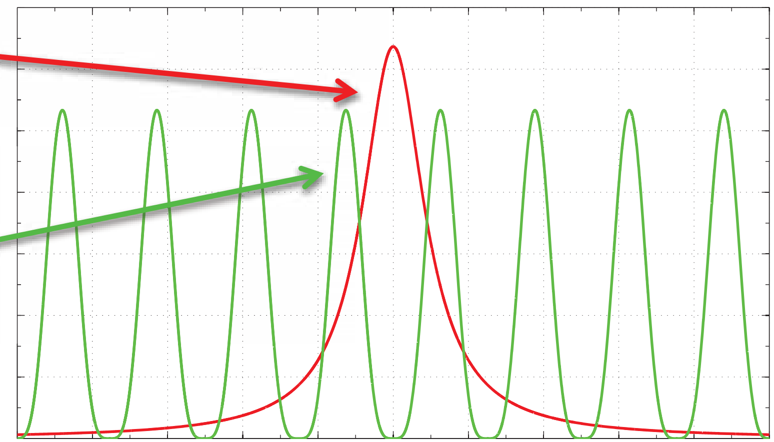

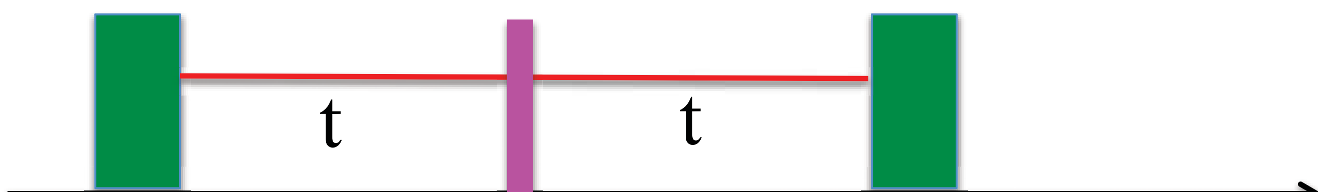

Quantum metrology with NV center: atomic-sized magnetometer

$$\hat{H} = \frac{1}{2}[\Omega + \beta(t)]\hat{\sigma}_z$$

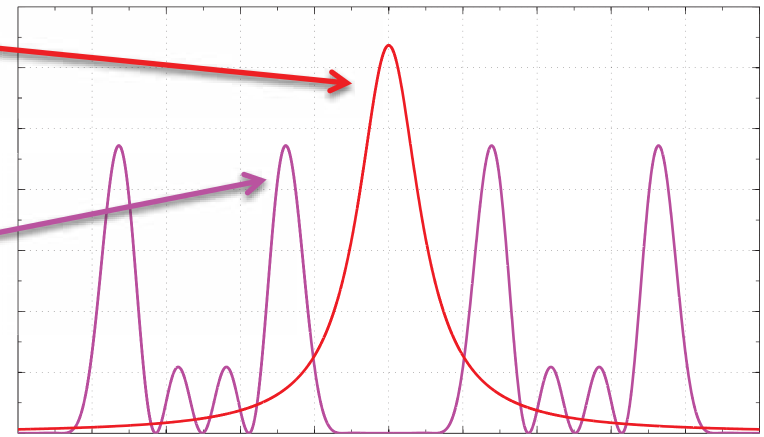

Decay of coherence:

$$W(t) \equiv e^{-\chi(t)}$$

$$\chi(t) = \int_0^\infty \frac{d\omega}{\pi} S(\omega) \frac{F(\omega t)}{\omega^2}$$

CPMG:

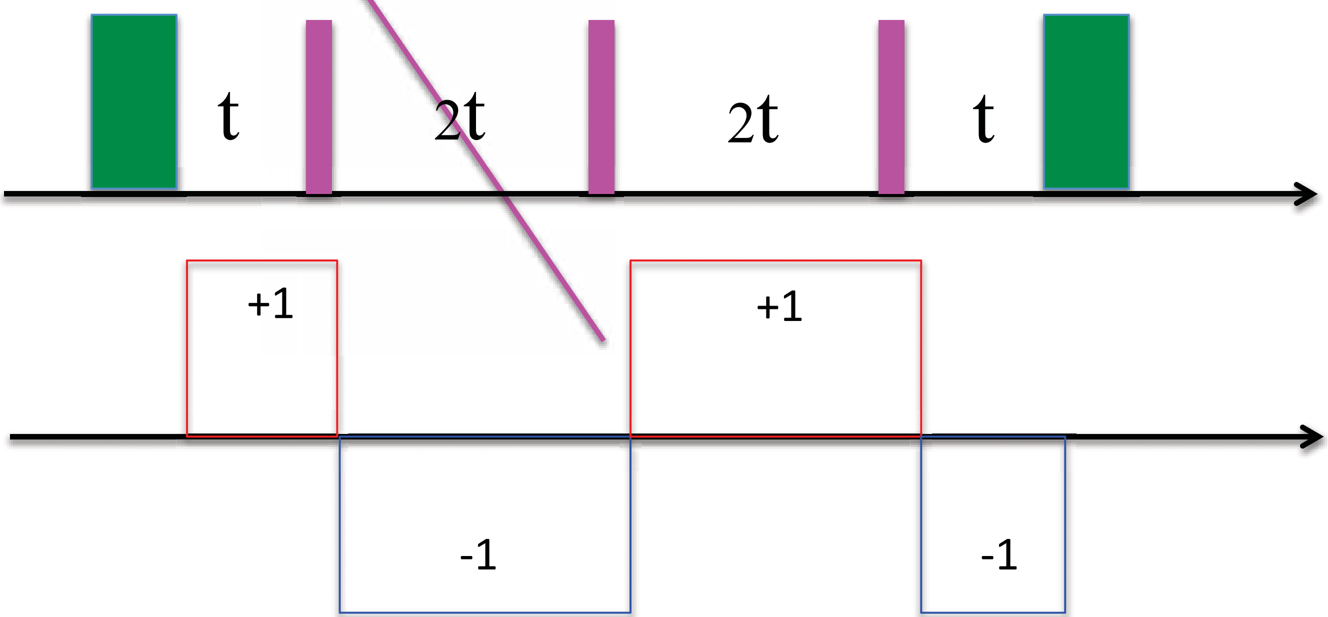

Quantum metrology with NV center: atomic-sized magnetometer

Nuclear Magnetic Resonance Spectroscopy on a (5-Nanometer)^3 Sample Volume
T. Staudacher *et al.*
Science **339**, 561 (2013);
DOI: 10.1126/science.1231675

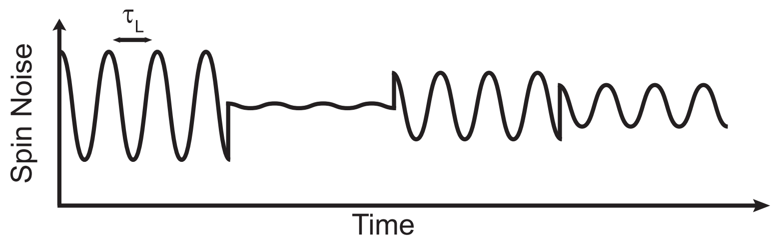

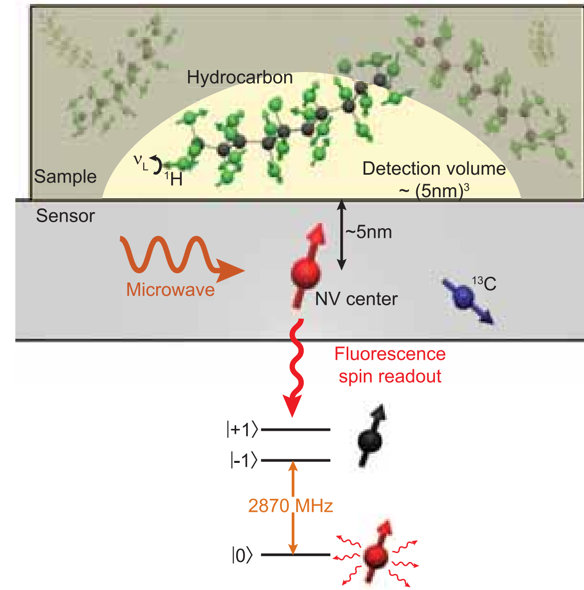

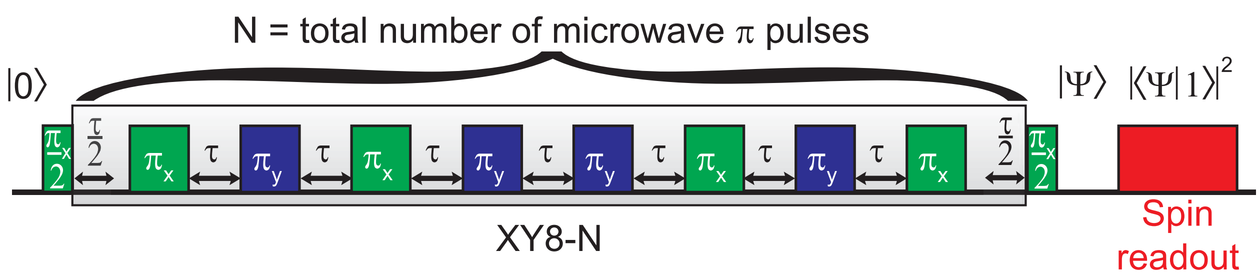

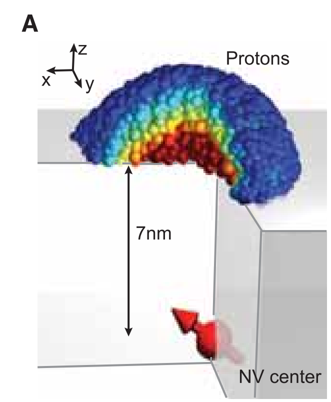

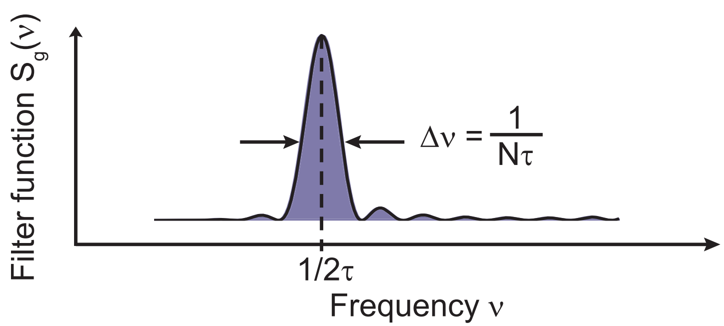

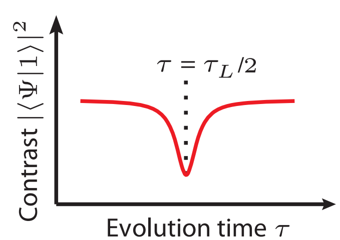

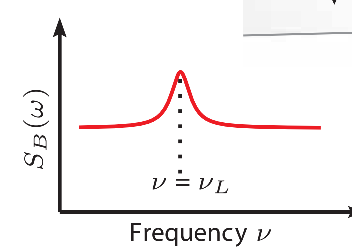

NV center as a quantum probe for biological applications

Pulse dynamical decoupling schemes: **Energy considerations**

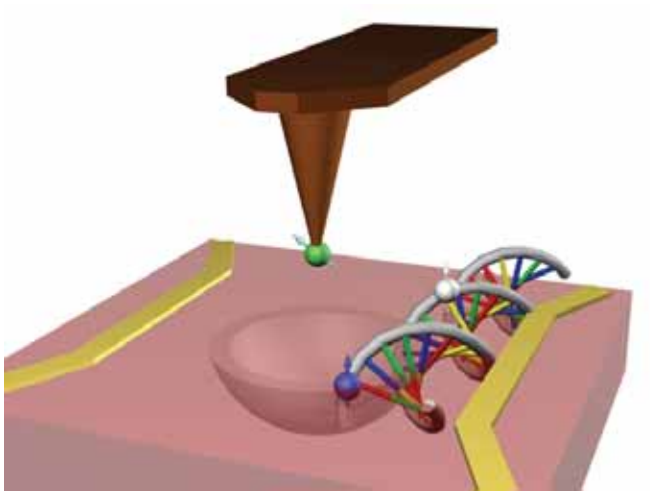

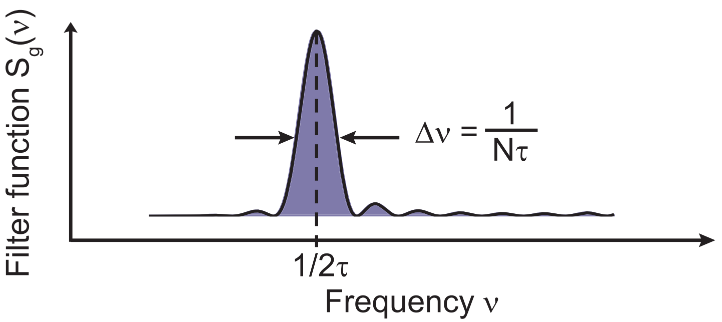

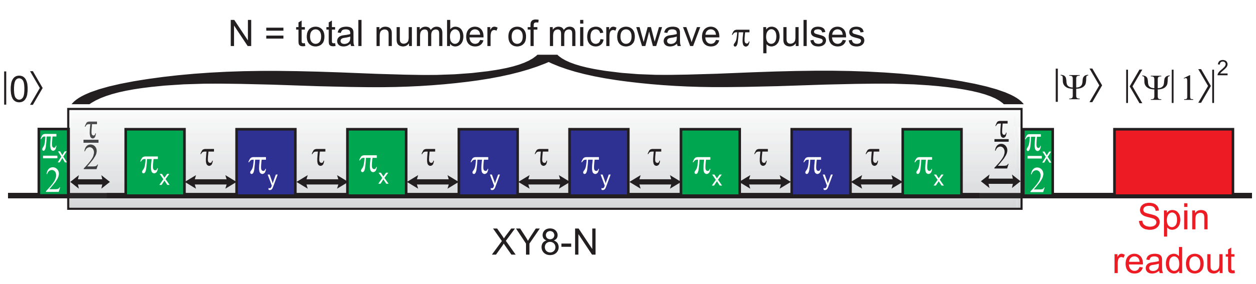

NV center as a tunable spectrometer with continuous driving

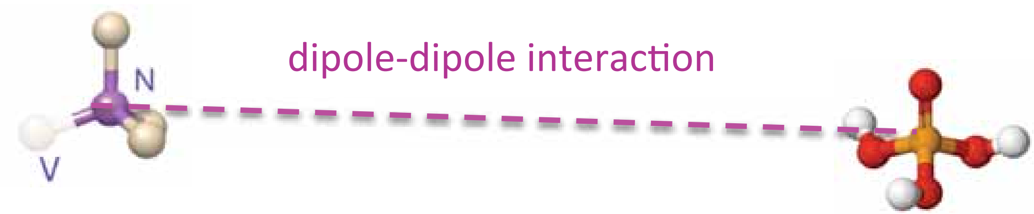

- Selective NV-nuclear spin coupling
  - ☞ Sensing nuclear spins: T_1
  - ☞ Readout nuclear spin state

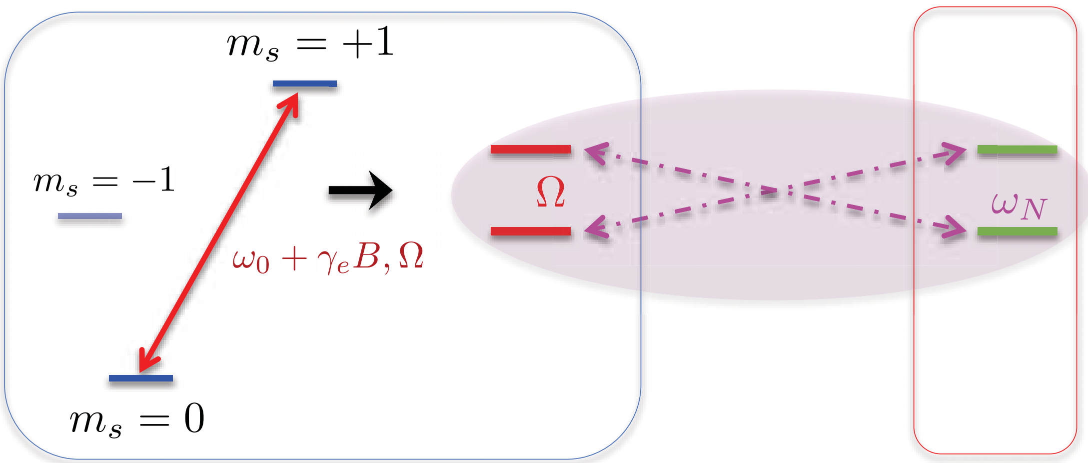

- Spin polarization exchange
  - ☞ Dynamical nuclear spin polarization

NV spectrometer

Target system

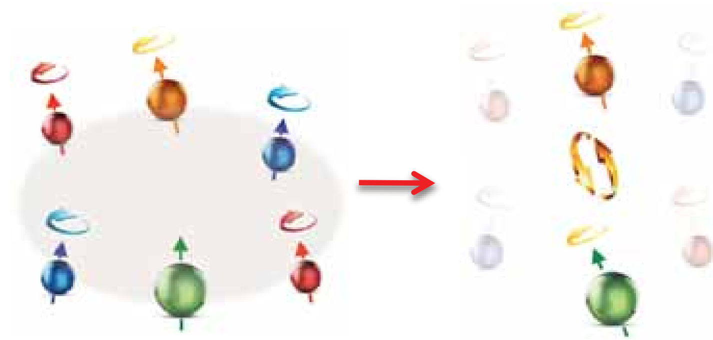

Hartmann-Hahn resonant condition (1962)

J.-M. Cai, F. Jelezko, M. B. Plenio, A. Retzker, arXiv:1112.5502, New J. Phys. 15, 013020 (2013)

Robust concatenated continuous driving

J.-M. Cai, B. Naydenov, R. Pfeiffer, L. P. McGuinness, K. D. Jahnke, F. Jelezko, M. B. Plenio, A. Retzker, arXiv:1111.0930, New J. Phys. **14**, 113023 (2012)

NV center as a tunable spectrometer with continuous driving

↓

Sensing nuclear or electron spins

Measure position of a single nucleus: Example

- Measurement on NV spin

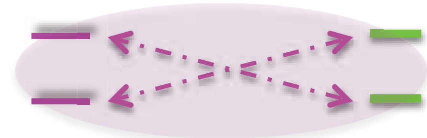

- Flip-flop process between spin sensor and target system

$$J = \frac{1}{4}\left(g\sqrt{3r_z^2+1}\right)\left(1-\left|\hat{h}\cdot\hat{b}\right|^2\right)^{1/2} \qquad S(t) = \frac{1}{2}+\frac{1}{4}\left[1+\cos\left(Jt\right)\right]$$

- Continuously drive hydrogen spins

$$\omega_{^{31}P} = 500kHz$$

$$\omega_{^{1}H} = 1235kHz$$

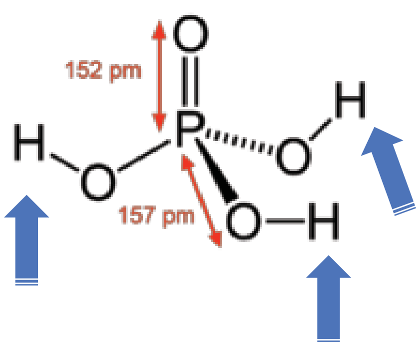

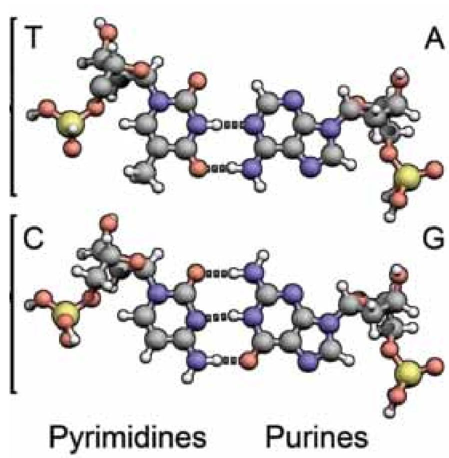

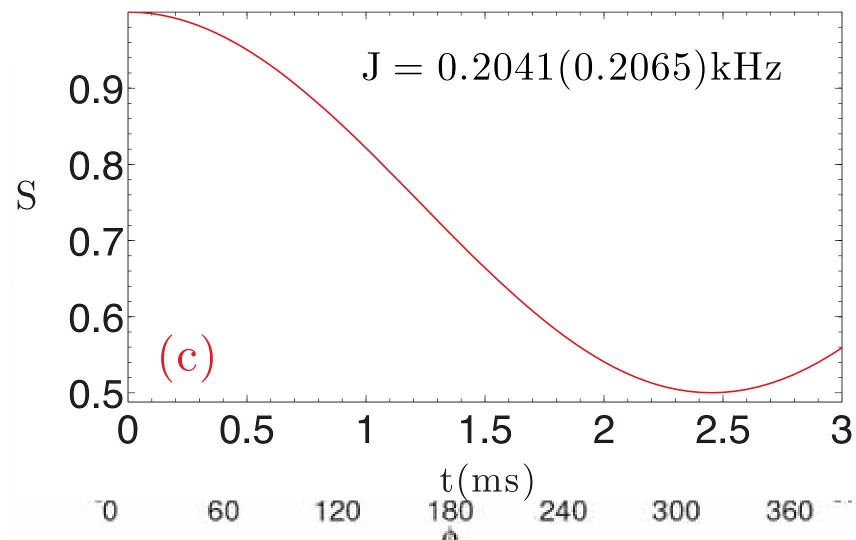

$$_{27}\Omega_{^{1}H} = 20kHz$$

$$g = -\frac{\hbar\mu_0\gamma_e\gamma_N}{4\pi r^3} \xrightarrow{r=5nm} 0.21kHz \rightarrow t = 3ms$$

Measure distance and alignment of a nuclear spin pair

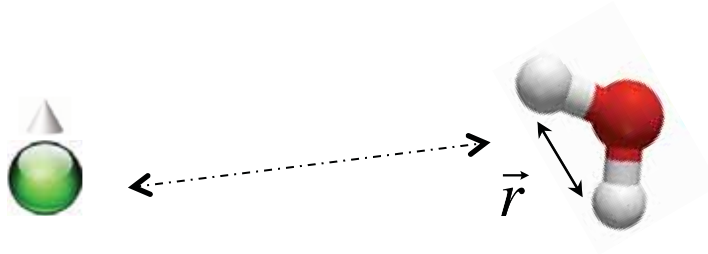

$$H_S = -\gamma_N \vec{B}\cdot(\vec{I}_1+\vec{I}_2) + g(\frac{1}{r^3})\left[\vec{I}_1\cdot\vec{I}_2 - 3\left(\vec{I}_1\cdot\hat{r}\right)\left(\vec{I}_2\cdot\hat{r}\right)\right]$$

- Magnetic field dependent energy spectrum of a spin pair

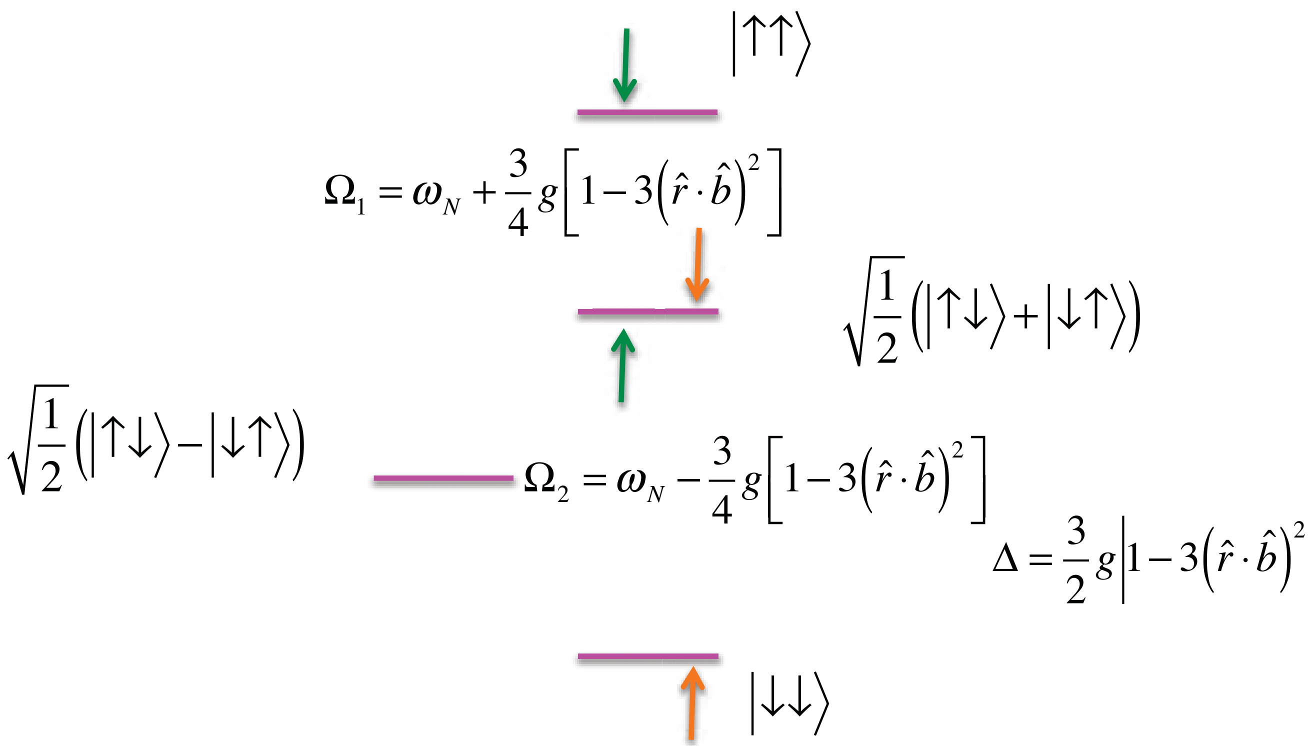

Measure distance and alignment of a nuclear spin pair

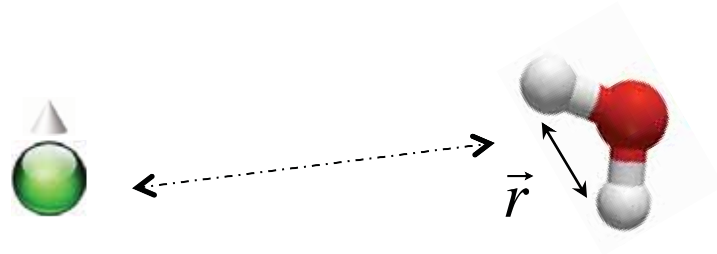

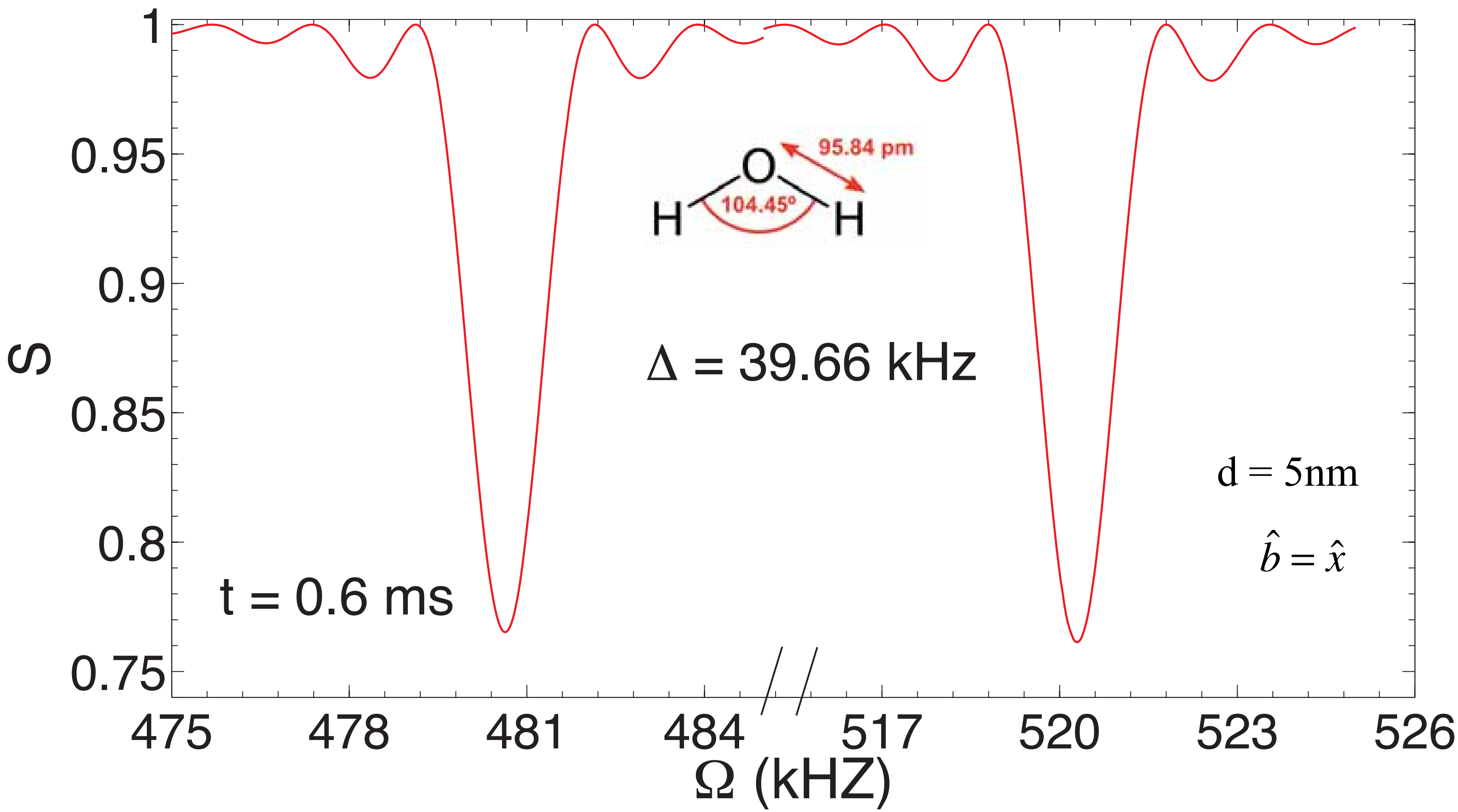

Measure distance and alignment of a nuclear spin pair

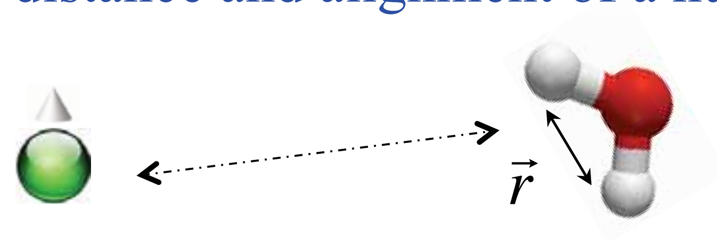

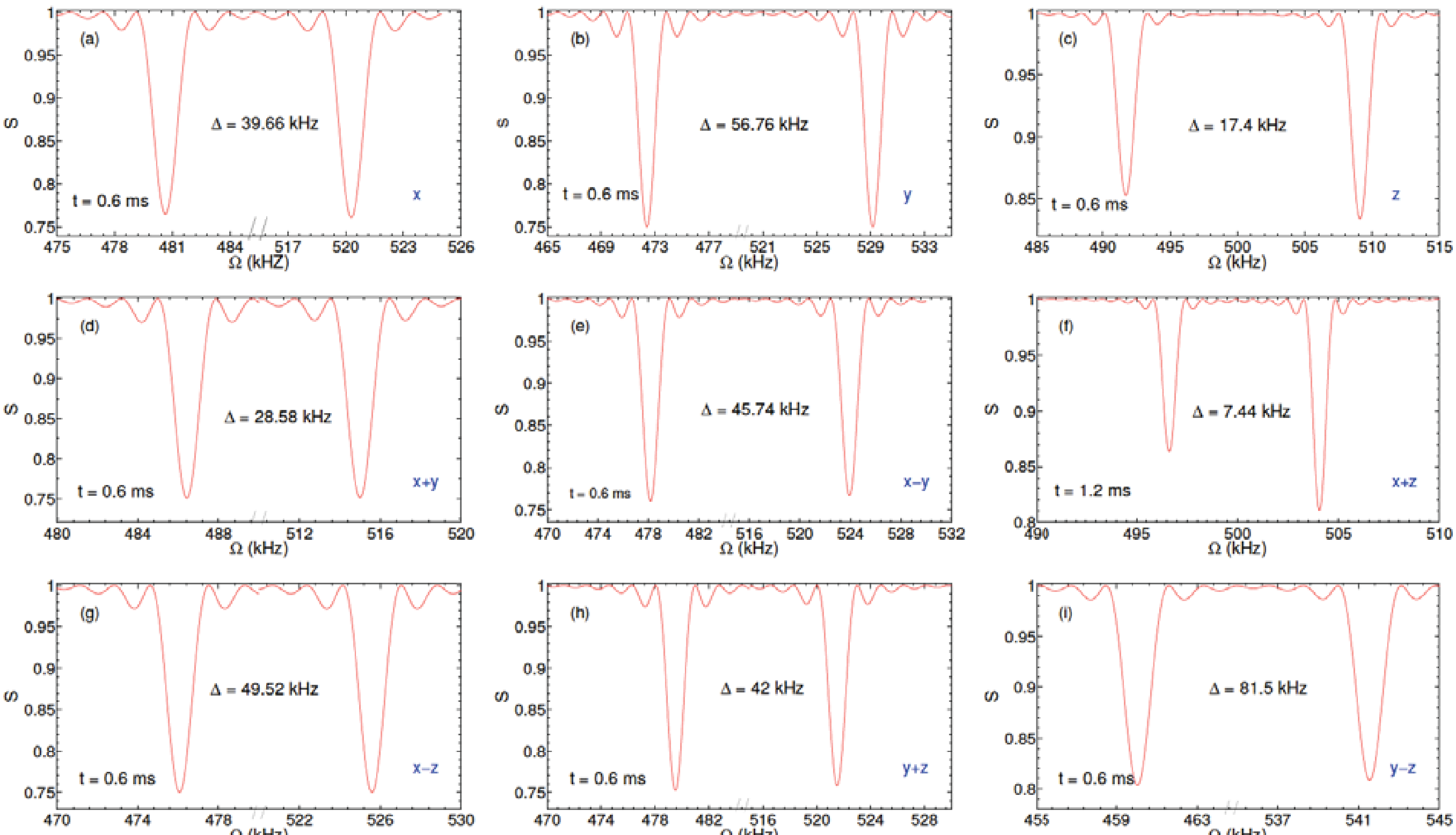

Measure distance between a pair of electron spins: organic spin labels

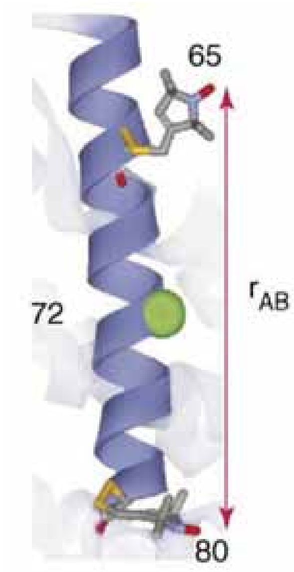

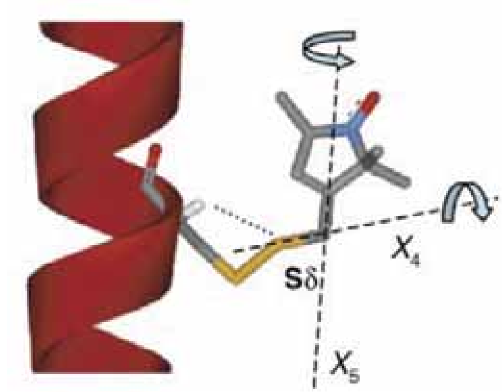

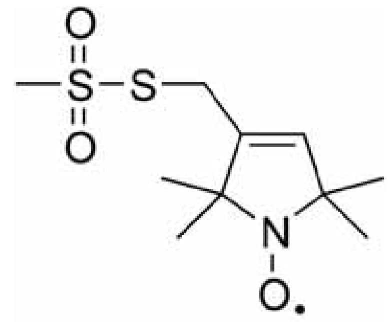

G. E. Fanucci and D. S. Cafiso, Recent advances and applications of site-directed spin labeling (2006)

- Wide applications:
  - Protein orientation
  - Protein dynamics
  - Distance measurements
  - Structural biology
- Determine intra and intermolecular distance: hard to go beyond 5 nm
  - Inhomogeneous broadening

Measure distance between a pair of electron spins: organic spin labels

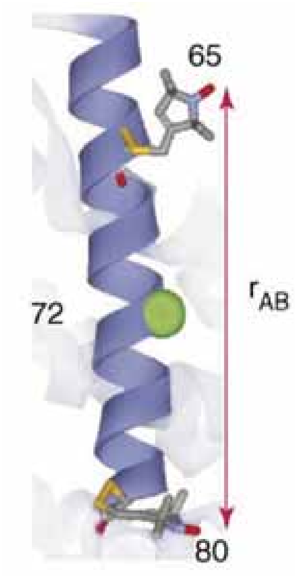

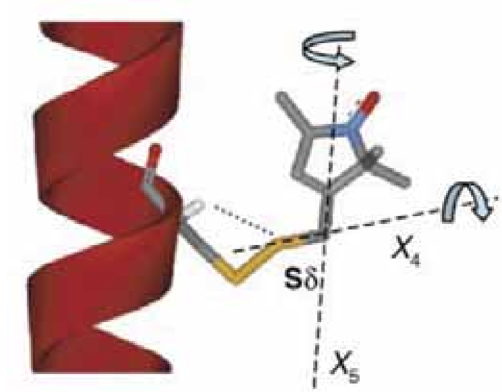

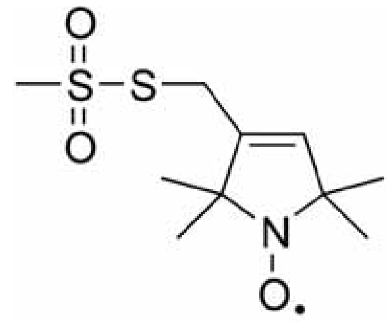

G. E. Fanucci and D. S. Cafiso, Recent advances and applications of site-directed spin labeling (2006)

- Continuously drive both NV center and label spins

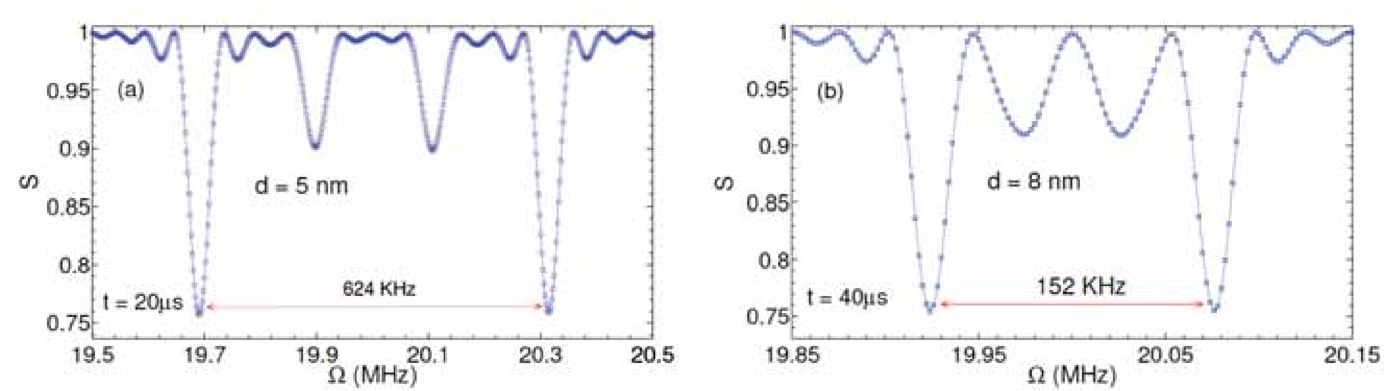

Monitor the charge recombination of radical pair

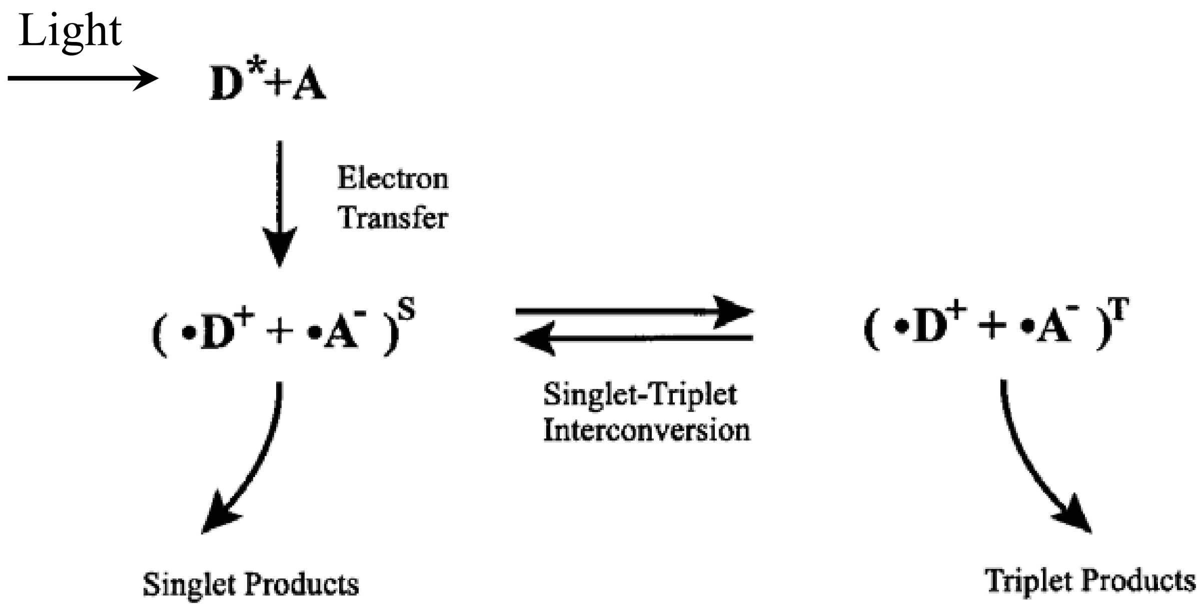

❖ Haberkorn Approach

$$\frac{d}{dt}\rho = -i[H,\rho] - \frac{1}{2}\left(L_S^\dagger L_S \rho + \rho L_S^\dagger L_S - 2L_S \rho L_S^\dagger\right) - \frac{1}{2}\left(L_T^\dagger L_T \rho + \rho L_T^\dagger L_T - 2L_T \rho L_T^\dagger\right)$$

$$L_S = k^{1/2}\left(Q_S \otimes |P\rangle\langle S|\right)$$
$$L_T = k^{1/2}\left(Q_T \otimes |P\rangle\langle S|\right)$$

U. E. Steiner and T. Ulrich, Chem. Rev. 89, 51-147 (1989)

Monitor the charge recombination of radical pair

Carotenoid-Porphyrin- Fullerene

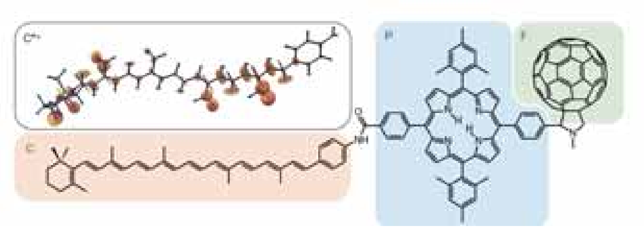

Peter Hore, Nature (2008)

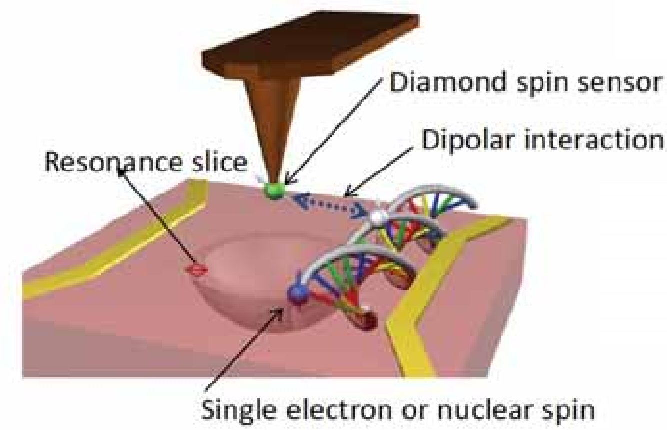

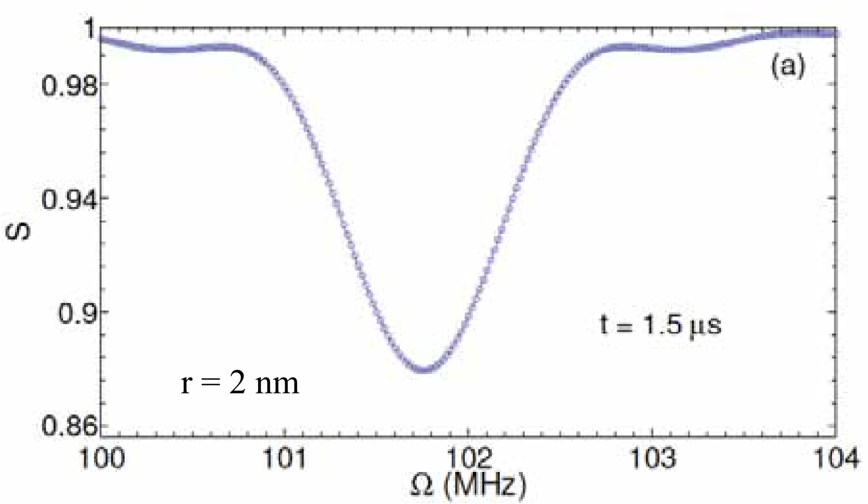

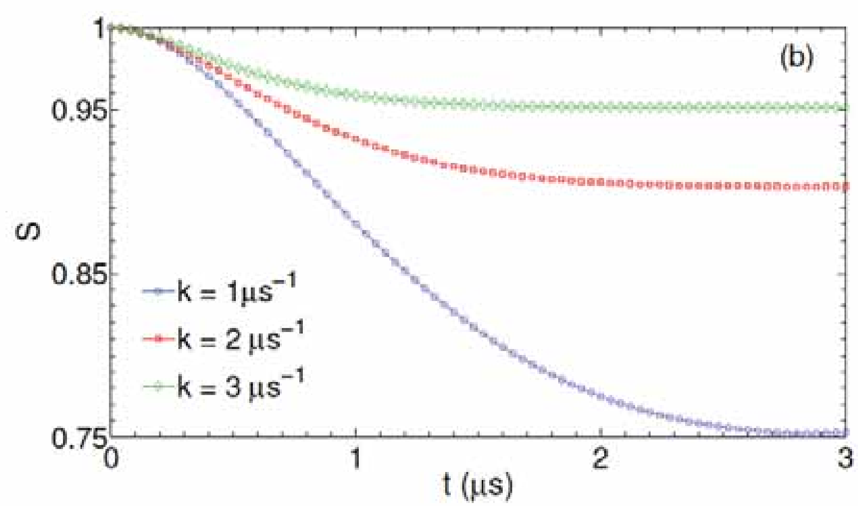

NV center as a control for external spins with continuous driving

External spin engineering: dynamical spin polarization

An unique feature of continuous driving as compared with pulse dynamical decoupling

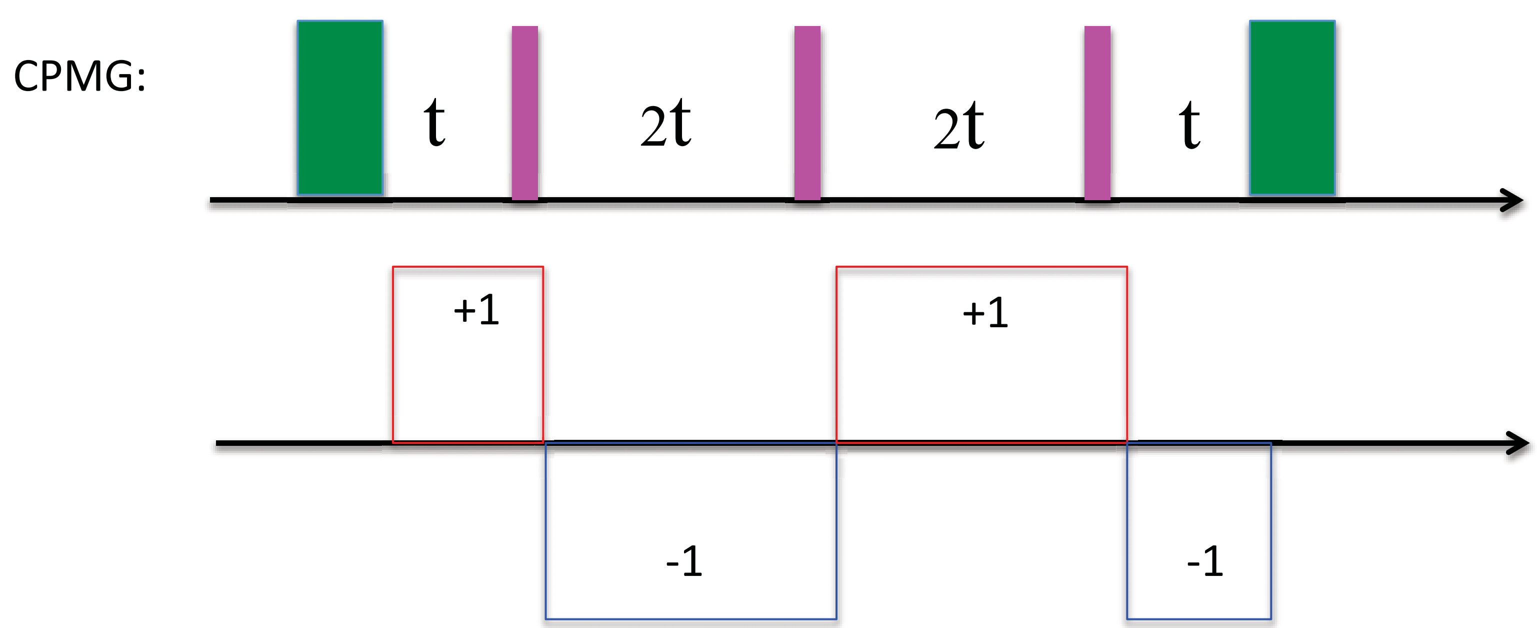

NV center for dynamical nuclear spin polarization

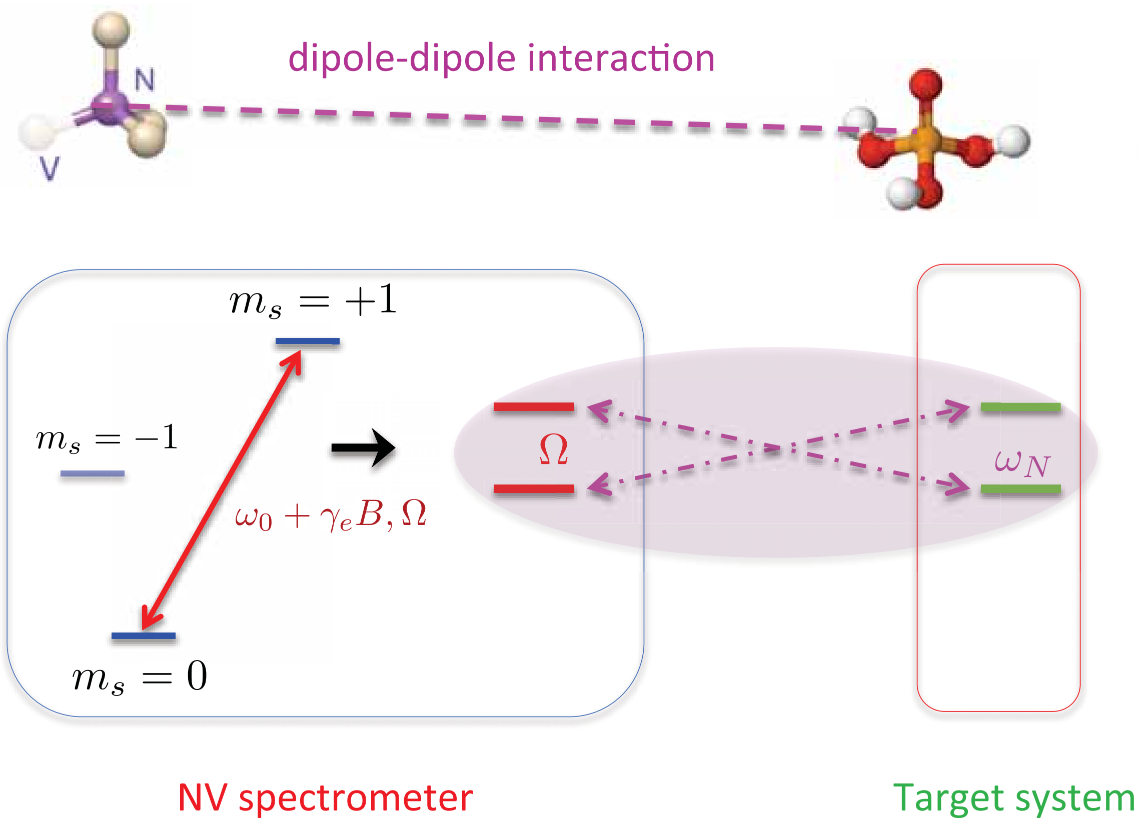

⚜ Spin polarization exchange

☞ Dynamical nuclear spin polarization

J.-M. Cai, F. Jelezko, M. B. Plenio, A. Retzker, arXiv:1112.5502, New J. Phys. 15, 013020 (2013)

Nuclear spin bath polarization: Experiment

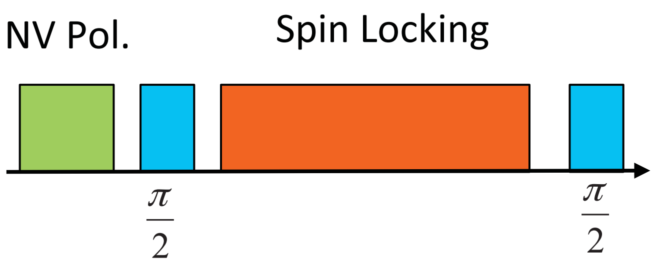

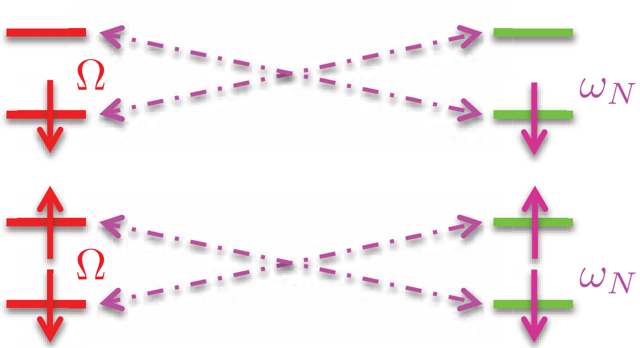

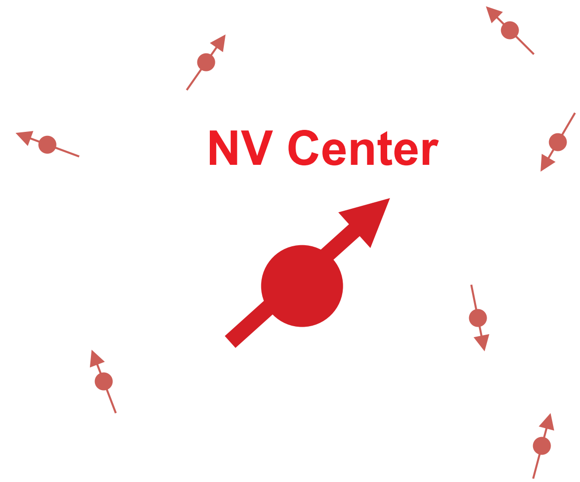

Paz London, Fedor Jelezko, J.-M. Cai et al, Submitted (2013)

Nuclear spin bath polarization: Experiment

- $B_0 = 0.5\mathrm{T}\ \ \omega(^{13}\mathrm{C}) = 5.8\ \mathrm{MHz}$

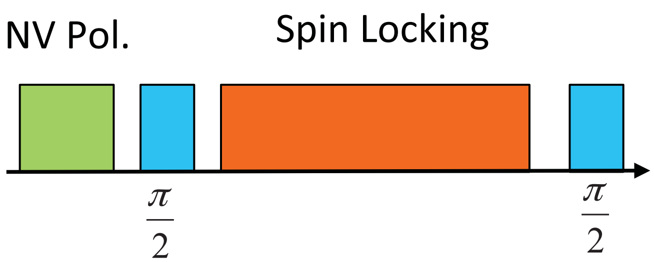

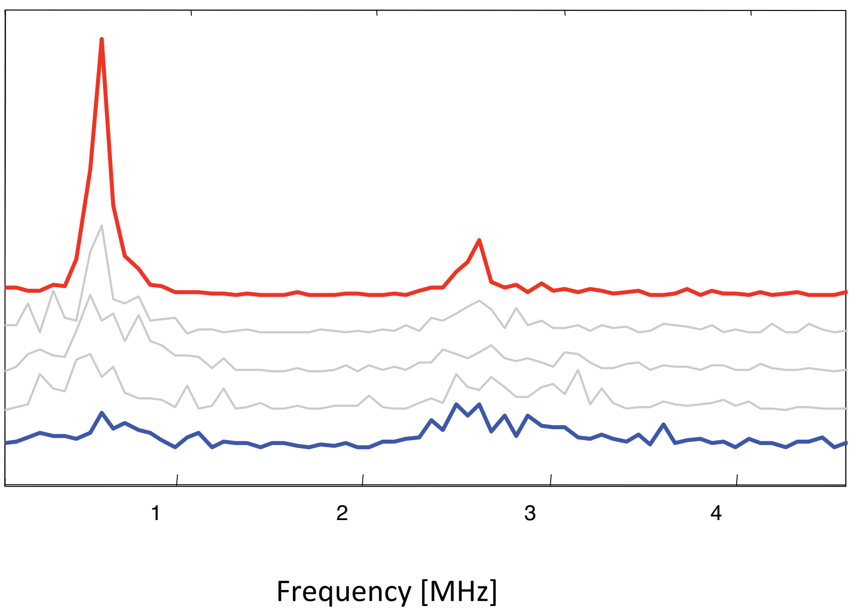

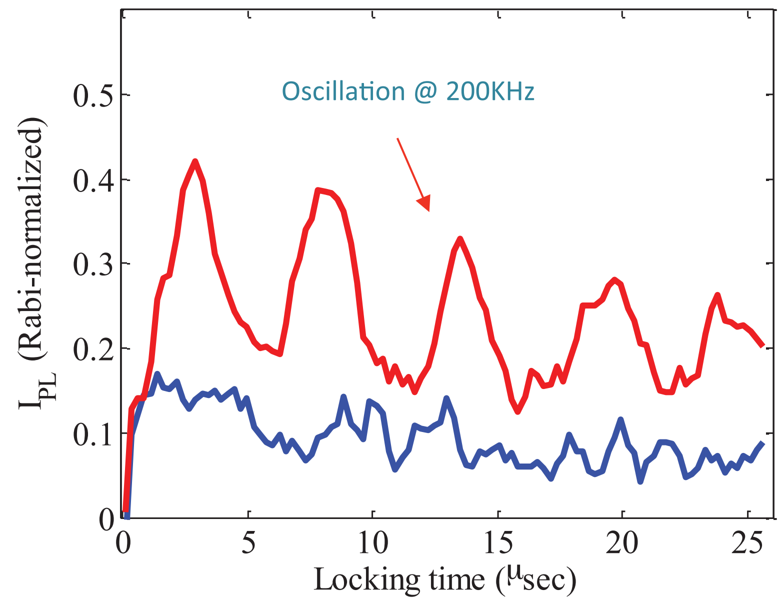

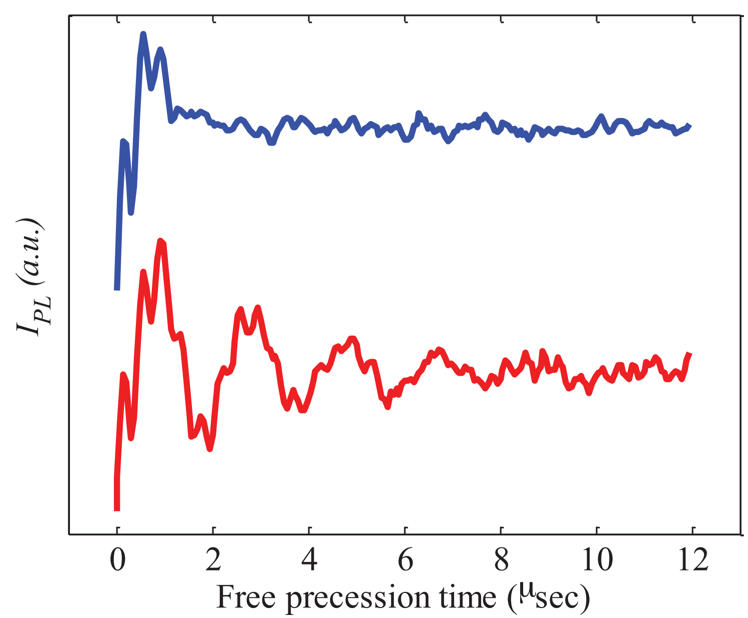

Paz London, Fedor Jelezko, J.-M. Cai et al, Submitted (2013)

NV centers for engineering many-body interactions

↓

Quantum simulation

Towards a large-scale quantum simulator on diamond surface: Introduction

Quantum superposition and entanglement

$$|\psi\rangle = c_1|\uparrow\uparrow\cdots\uparrow\uparrow\rangle + c_2|\uparrow\uparrow\cdots\uparrow\downarrow\rangle\cdots+\cdots c_N|\downarrow\downarrow\cdots\downarrow\downarrow\rangle$$

N=2^{300} for 300 spins

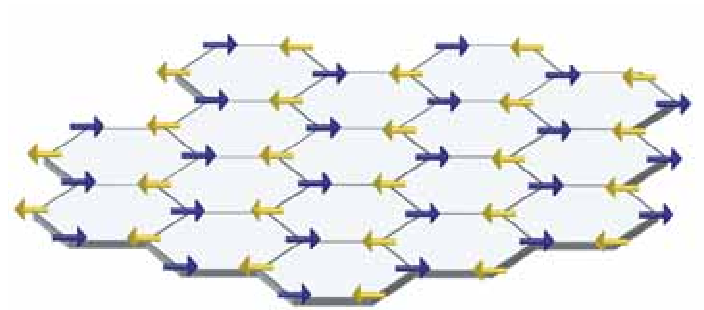

©E. Edwards

Simulating Physics with Computers

Richard P. Feynman

Department of Physics, California Institute of Technology, Pasadena, California 91107

Received May 7, 1981

be understood very well in analyzing the situation. And I'm not happy with all the analyses that go with just the classical theory, because nature isn't classical, dammit, and if you want to make a simulation of nature, you'd better make it quantum mechanical, and by golly it's a wonderful problem, because it doesn't look so easy. Thank you.

Quantum simulation beyond classical methods

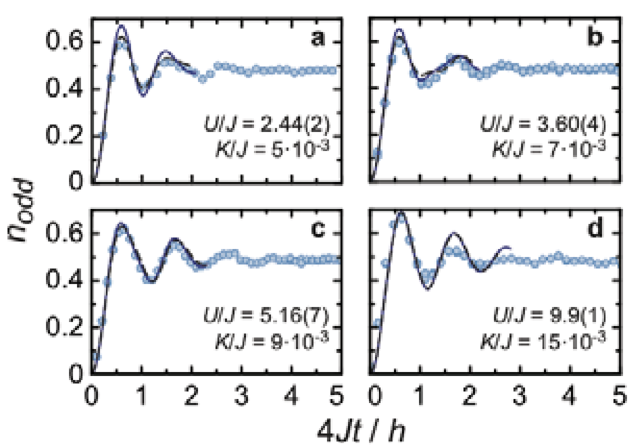

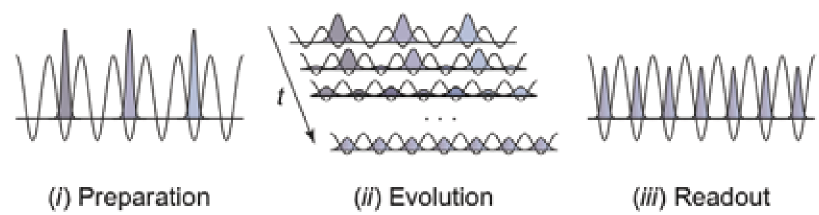

I. Bloch, Nature Physics (2012)

Towards a large-scale quantum simulator on diamond surface: Introduction

- Optical lattice

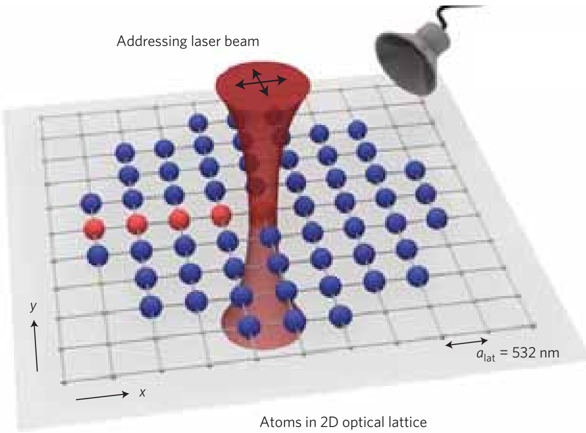

- Trapped ions

Britton et al, Science (2012)

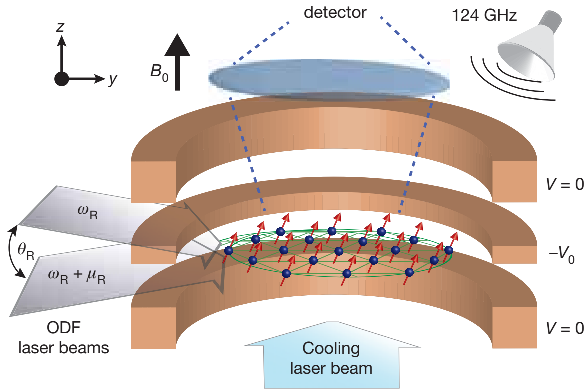

- Photonic system

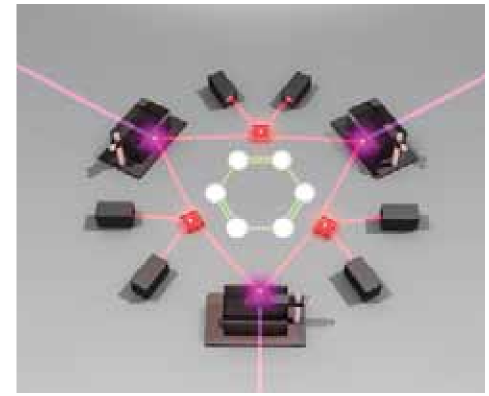

- Superconducting circuit

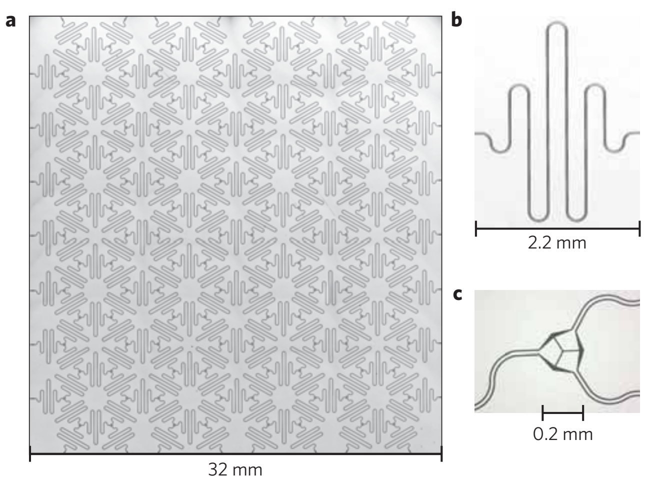

Nature Physics insight: Quantum Simulation (2012)

Initialization

Hamiltonian engineering

Detection

Low temperature and pressure

Extremely hard to scale

Diamond-based quantum simulator: architecture

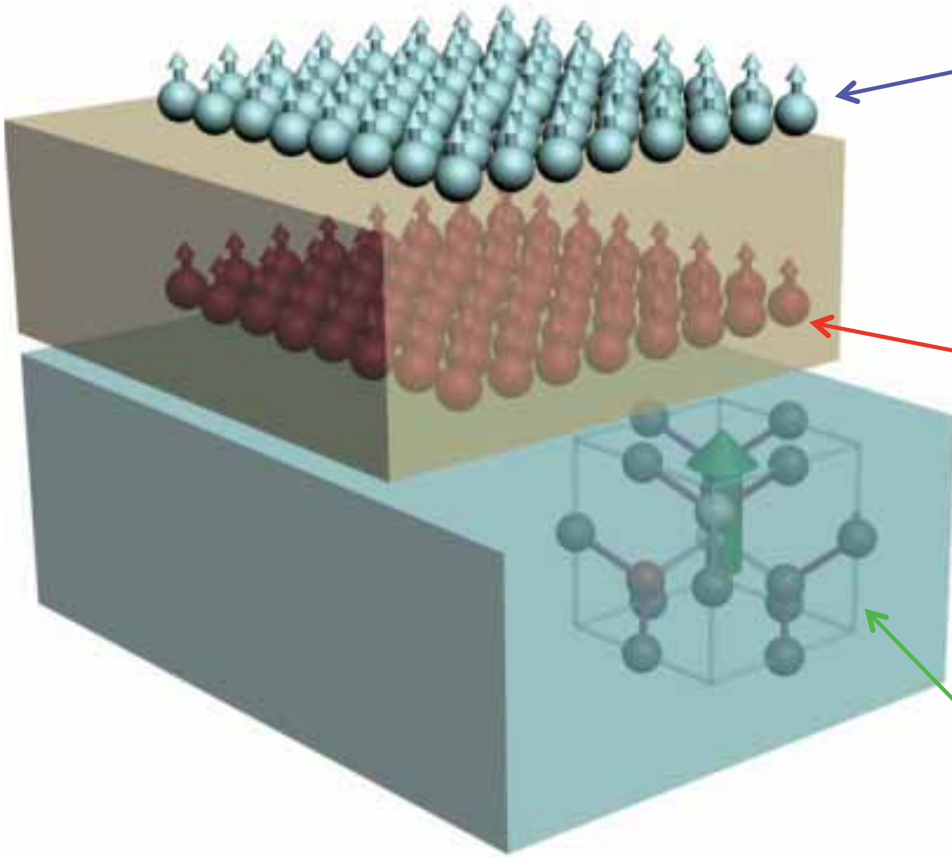

Fluorine nuclear spins (directly linked to diamond or linked to a graphene sheet)

Electron and nuclear spin arrays in diamond (P donor, ^{13}C)

NV center in nuclear spin free ^{12}C diamond

(used for initiaizaiton and readout via dipole dipole coupling to spin arrays)

Slide from Fedor Jelezko

Diamond-based quantum simulator: architecture

(a) (111) surface

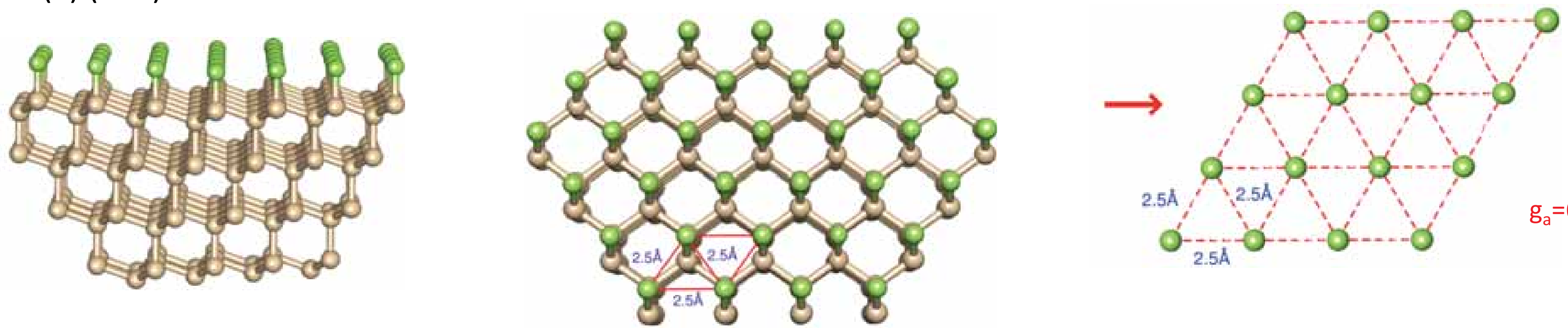

g_a=6.8kHz

(b) (100) surface

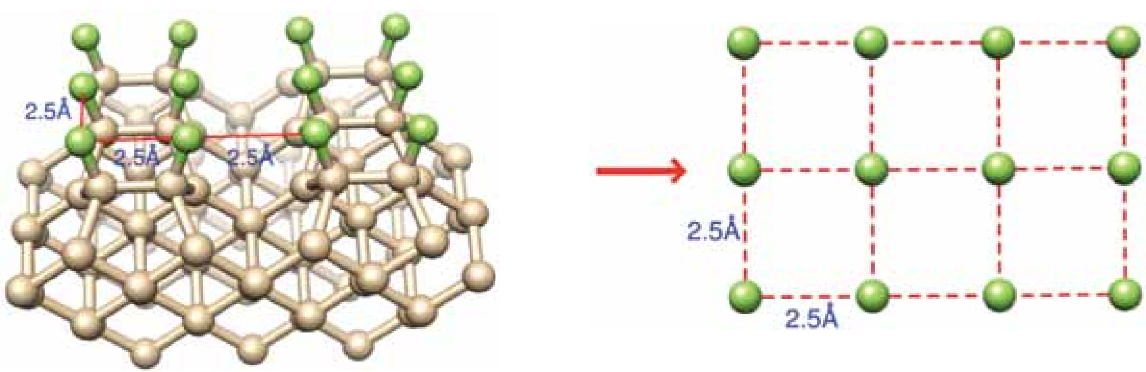

J.-M. Cai, Alex Retzker, Fedor Jelezko, Martin B. Plenio, arXiv:1208.2874, Nature Physics 9, 168–173 (2013).

Diamond-based quantum simulator: architecture

(c) Fluorographene

Novoselov and Gein, Small (2010)

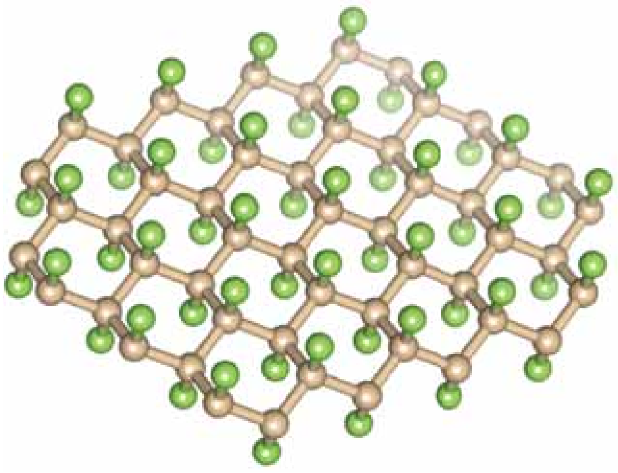

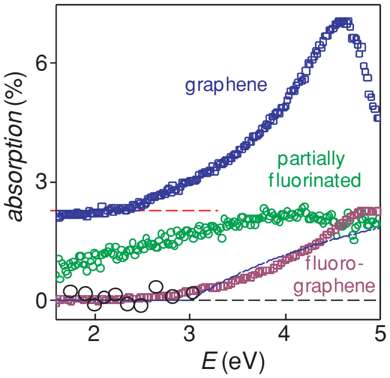

(d) Controllable growth of nuclear spin layer in diamond

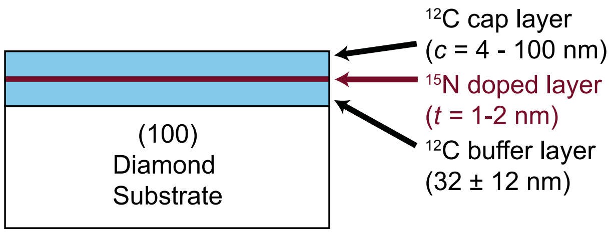

CVD-overgrowth

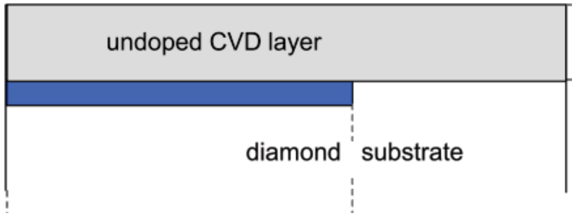

Jörg Wrachtrup (Stuttgart) 2012

David D. Awschalom (UCSB), APL (2012)

Nuclear spin quantum simulator on diamond surface

$$H_{\mathrm{F}} = \sum_i \gamma_N \mathrm{B} \mathbf{s}_i^z + \frac{\mu_0}{4\pi} \sum_{i,j} \frac{\gamma_N^2}{r_{ij}^3} \left[\mathbf{s}_i \cdot \mathbf{s}_j - 3 \left(\mathbf{s}_i \cdot \hat{\mathbf{r}}_{ij} \right) \left(\mathbf{s}_j \cdot \hat{\mathbf{r}}_{ij} \right) \right] + 2\Omega_F \cos\left[(\gamma_N \mathrm{B} - \omega_F) t \right] \sum_i \mathbf{s}_i^x$$

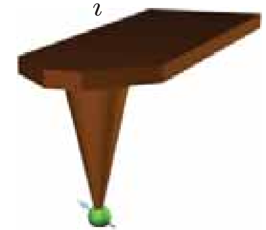

$$H_{\mathrm{F}} = \sum_i \left(\omega_F \mathbf{s}_i^z + \Omega_F \mathbf{s}_i^x \right) + \sum_{i,j} g_{ij} \left[\mathbf{s}_i^z \cdot \mathbf{s}_j^z - \Delta (\mathbf{s}_i^x \cdot \mathbf{s}_j^x + \mathbf{s}_i^y \cdot \mathbf{s}_j^y) \right]$$

$$\equiv H_S + \Omega_F \sum_i \mathbf{s}_i^x$$

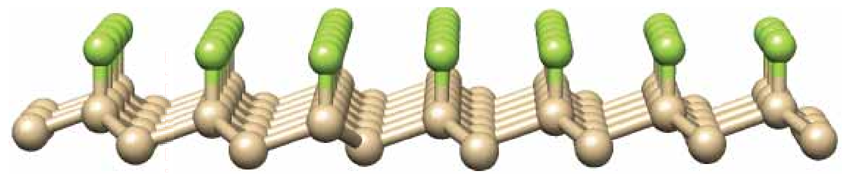

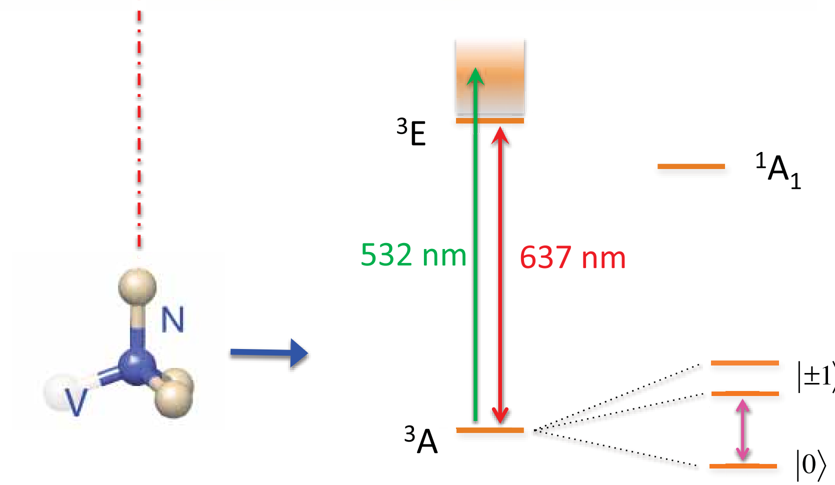

$$H_{\mathrm{NV-F}} = \frac{\mu_0}{4\pi} \sum_i \frac{\gamma_e \gamma_N}{r_i^3} \left[\mathbf{S} \cdot \mathbf{s}_i - 3 \left(\mathbf{S} \cdot \hat{r} \right) \left(\mathbf{s}_i \cdot \hat{r} \right) \right].$$

Nuclear spin quantum simulator on diamond surface: Frustrated Quantum Magnetism

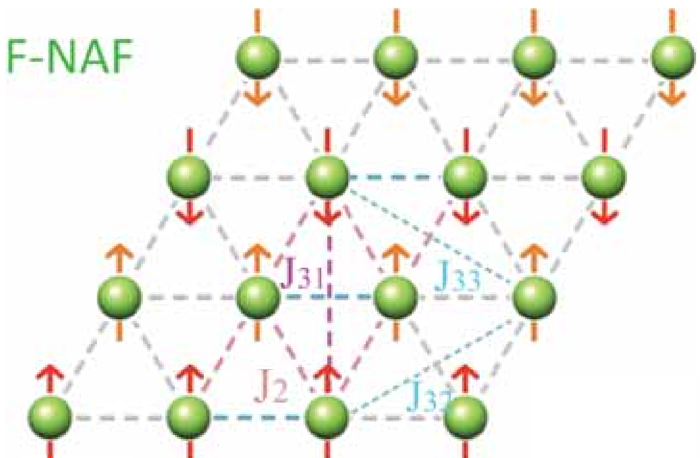

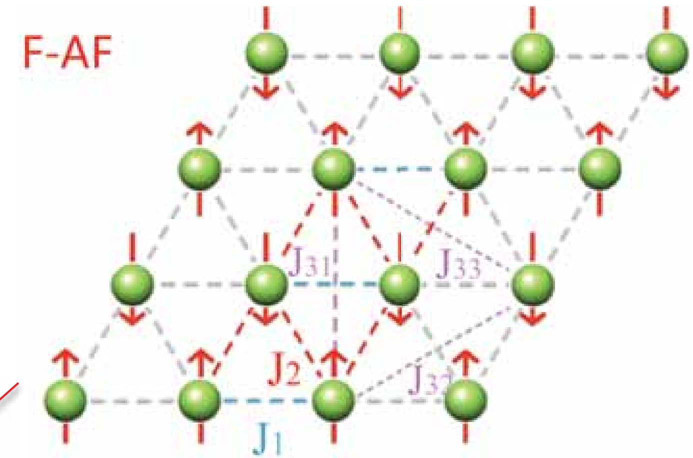

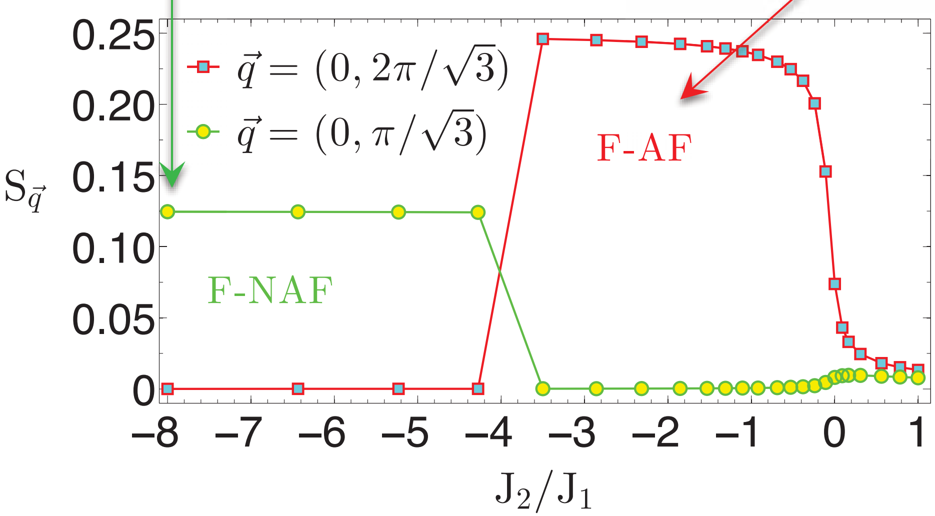

Spin structure factor:

$$S_{\vec{q}} = \sum_{\langle kl \rangle} \left[e^{i\vec{q}\cdot(\vec{r}_k - \vec{r}_l)} S_k^z S_l^z \right]$$

Nuclear spin quantum simulator on diamond surface: Supersolid

Hardcore boson model: $$H_b = \sum_{\langle i,j\rangle}\left(V_{ij}n_in_j - t_{ij}\left(a_i^\dagger a_j + a_i a_j^\dagger\right)\right) + \mu\sum_i n_i$$

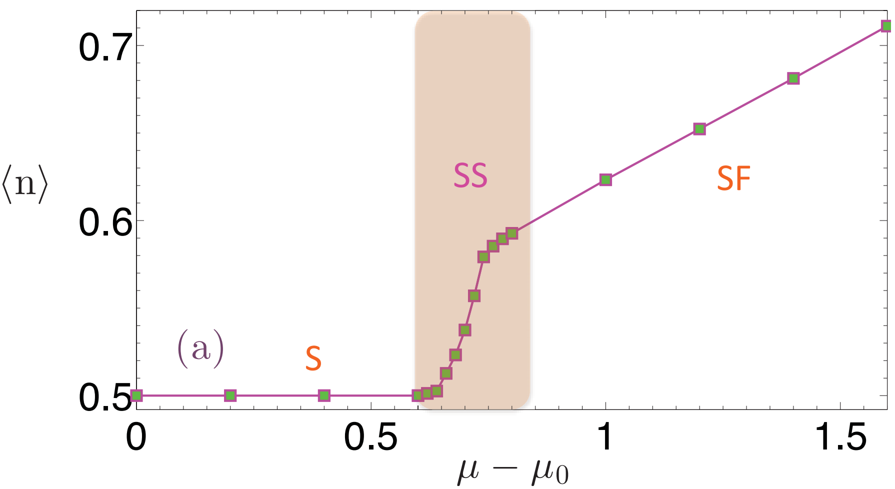

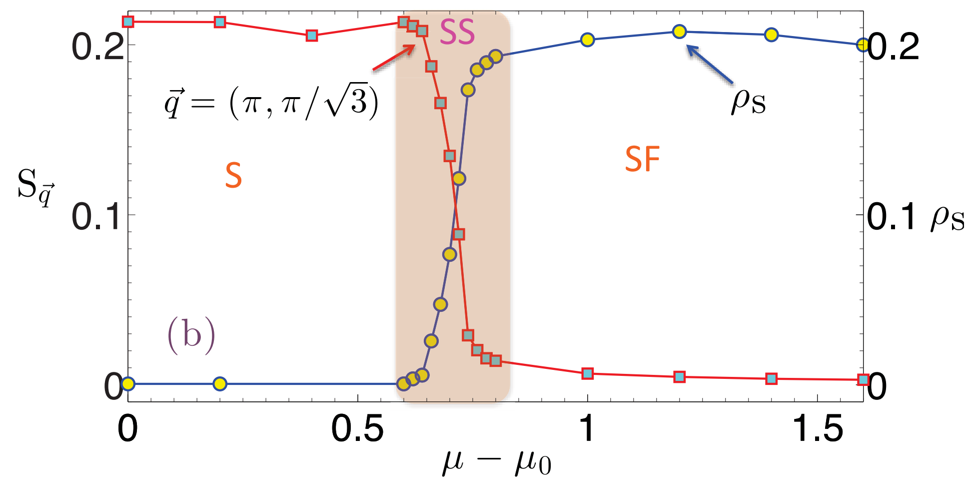

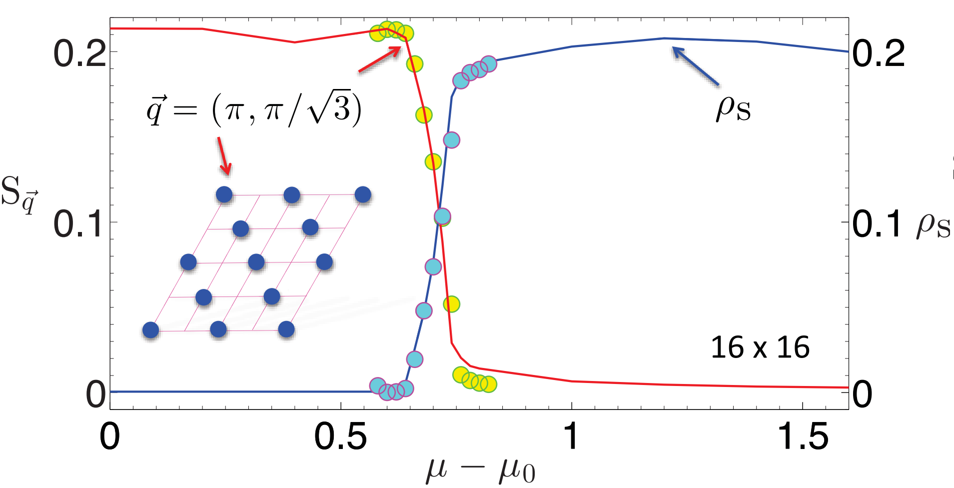

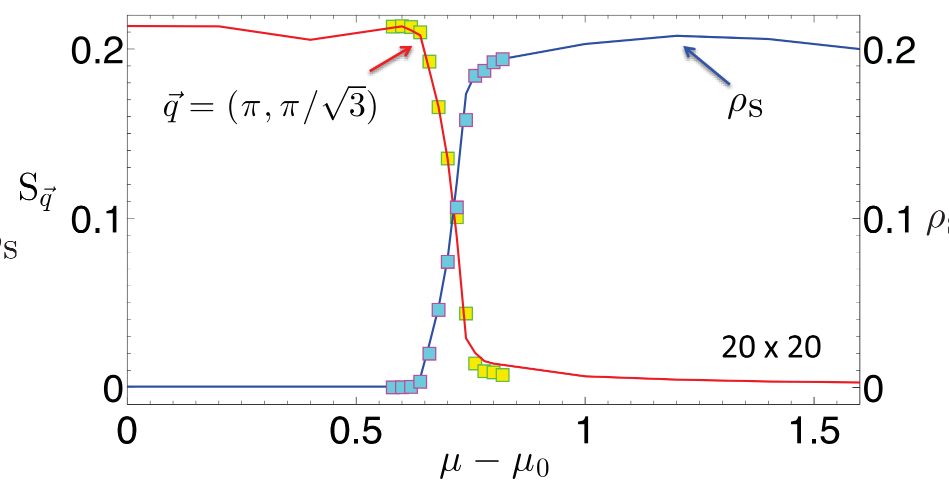

Towards a large-scale quantum simulator on diamond surface: Detection

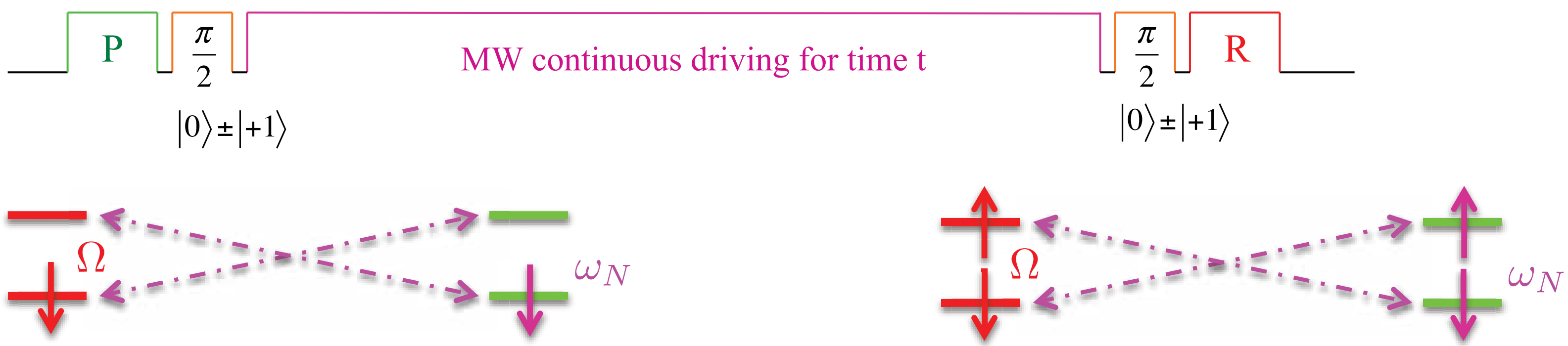

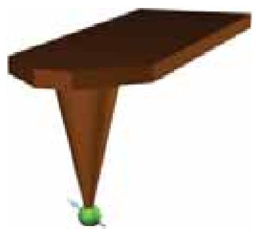

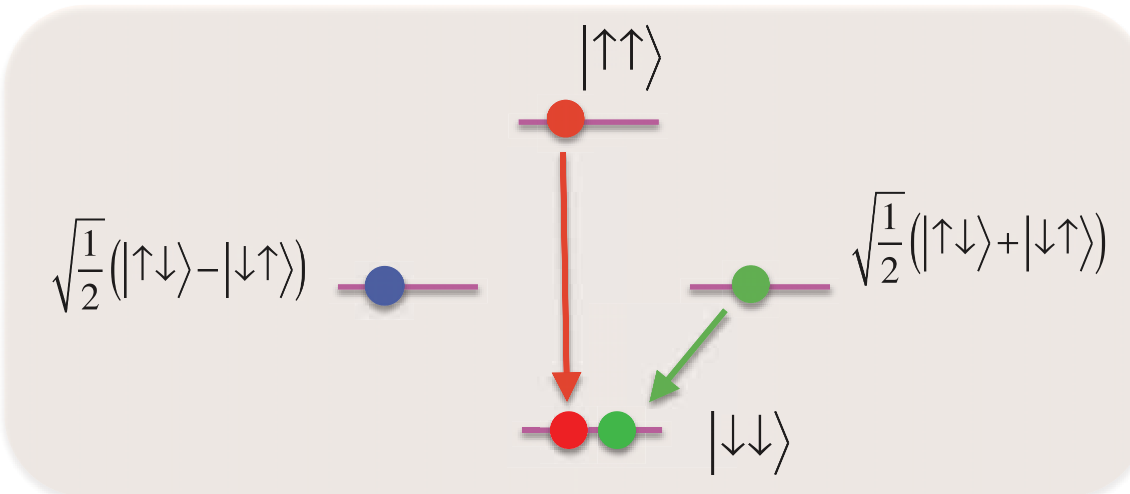

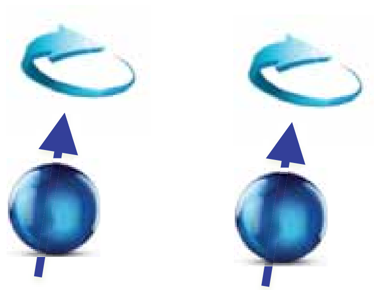

$$P_-^+ = \tau^2 \sum_i \sum_j (g_i^\perp g_j^\perp)\langle \tilde{s}_i^+ \tilde{s}_j^- \rangle = \tau^2 \sum_i (g_i^\perp)^2 P_i^{\tilde{\uparrow}} + \tau^2 \sum_{(i,j),i\neq j} (g_i^\perp g_j^\perp)\langle \tilde{s}_i^+ \tilde{s}_j^- + \tilde{s}_i^- \tilde{s}_j^+ \rangle,$$

$$P_+^- = \tau^2 \sum_i \sum_j (g_i^\perp g_j^\perp)\langle \tilde{s}_i^- \tilde{s}_j^+ \rangle = \tau^2 \sum_i (g_i^\perp)^2 P_i^{\tilde{\downarrow}} + \tau^2 \sum_{(i,j),i\neq j} (g_i^\perp g_j^\perp)\langle \tilde{s}_i^+ \tilde{s}_j^- + \tilde{s}_i^- \tilde{s}_j^+ \rangle$$

Towards a large-scale quantum simulator on diamond surface: Detection

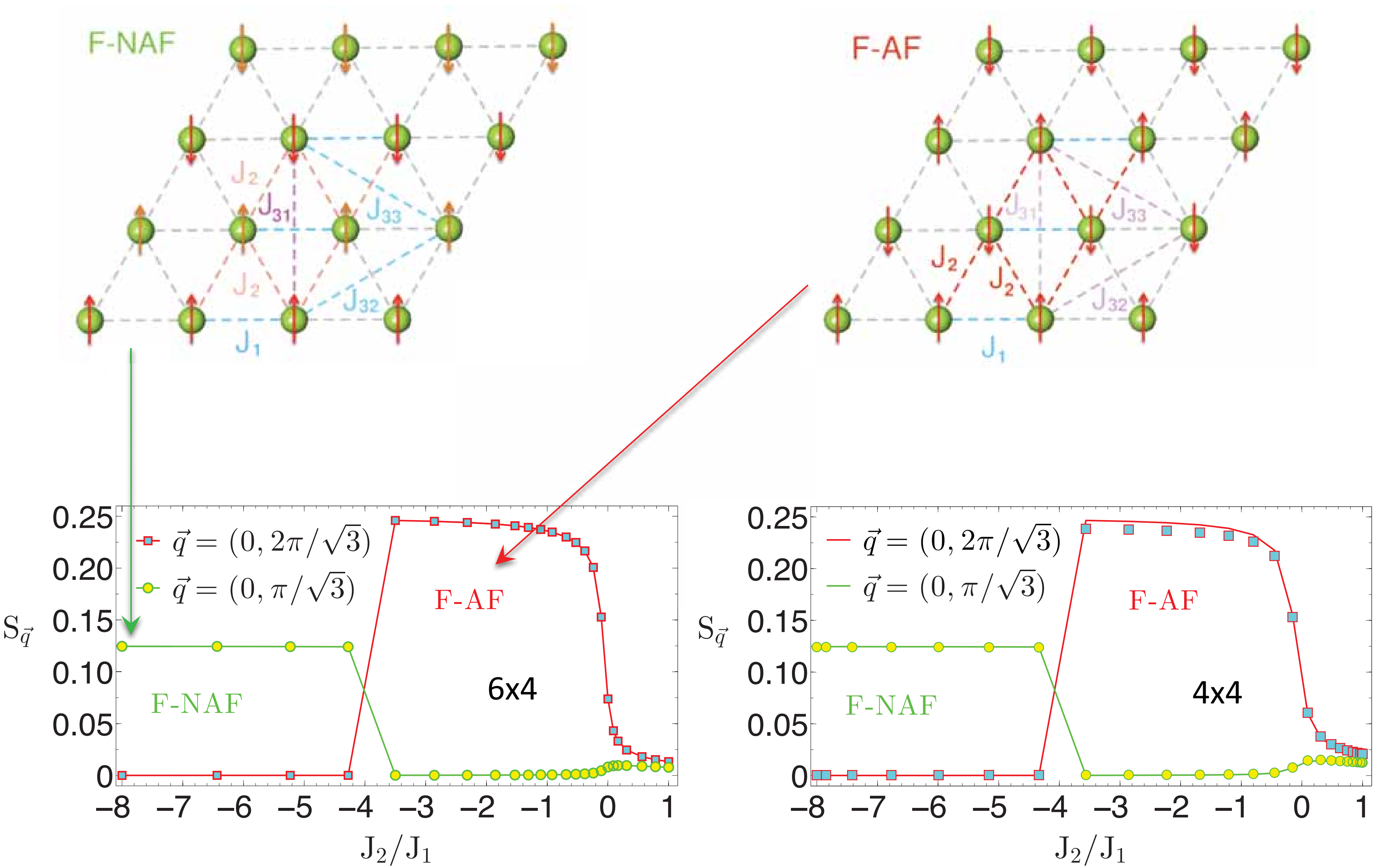

Thanks for your attention!